IEEE Access
Multidisciplinary | Rapid Review | Open Access Journal

Received 31 August 2022, accepted 23 September 2022, date of publication 3 October 2022, date of current version 10 October 2022.

Digital Object Identifier 10.1109/ACCESS.2022.3211388

RESEARCH ARTICLE

Robust QoT Assured Resource Allocation in Shared Backup Path Protection Based EONs

VENKATESH CHEBOLU[1], SADANANDA BEHERA[2], AND GOUTAM DAS[1], (Member, IEEE)
[1]G.S Sanyal School of Telecommunications, Indian Institute of Technology Kharagpur, Kharagpur 721302, India
[2]KIOS Research and Innovation Center of Excellence, University of Cyprus, 2109 Aglantzia, Nicosia, Cyprus

Corresponding author: Venkatesh Chebolu (venkat.chebolu@iitkgp.ac.in)

ABSTRACT Survivability is mission-critical for elastic optical networks (EONs) as they are expected to carry an enormous amount of data. In this paper, we consider the problem of designing shared backup path protection (SBPP) based EON that facilitates the minimum quality-of-transmission (QoT) assured allocation against physical layer impairments (PLIs) under any single link/shared risk link group (SRLG) failure for static and dynamic traffic scenarios. In general, the effect of PLIs on lightpath varies based on the location of failure of a link as it introduces different active working and backup paths. To address these issues in the design of SBPP EON, we formulate a mixed integer linear programming (MILP) based robust optimization framework for static traffic with the objective of minimizing overall fragmentation. In this process, we use the efficient robust bitloading technique for spectrum allocation where each frequency slot of a request is assigned with different modulation format. In addition, we propose novel SBPP-impairment aware (SBPP-IA) algorithm considering the limitations of MILP for larger networks. For this purpose, we introduce a novel sorting technique named most congested working-least congested backup first (MCW-LCBF) to sort the given set of requests. Next, we employ our SBPP-IA algorithm for dynamic traffic scenario and compare it with existing algorithms in terms of different QoT parameters. Further, we guarantee the QoT of existing requests while allocating each new request without reserving any margin. We demonstrated through simulations that our study provides 33.94-41.02% more QoT guaranteed requests compared to existing ones at 70 Tbps traffic load.

INDEX TERMS Elastic optical networks, fragmentation, mixed integer linear programming, physical layer impairments, quality of transmission, shared backup path protection.

I. INTRODUCTION

Elastic optical networks (EONs) have emerged as a potential candidate to replace the existing wavelength division multiplexed networks due to their superior attributes in terms of huge data transportation and high spectrum efficiency [1]. In general, optical networks suffer from unexpected link and shared risk link group (SRLG) failures which may cause the failure of multiple lightpaths resulting in immense loss of data and revenue. In order to overcome this, it is imperative to design a survivable EON that enables the normal operation of the network during link/SRLG failures. Several EON based protection techniques, namely, span restoration, p-cycles, dedicated protection, shared backup path protection (SBPP) etc. are proposed in the literature [2]. Among all, SBPP has been widely adopted as it offers major benefits such as effective protection capacity sharing, fast recovery, and less complexity [2]. Therefore, in this work, we focus on SBPP based EON.

Routing and spectrum assignment (RSA) is an integral part of network planning wherein a request is assigned a route and wavelength(s). In a transparent optical network, the transmission quality of a lightpath is affected by various physical layer impairments (PLIs). Note that, existing works related to SBPP based EON [3], [4], [5], [6], [7], [8], [9], [10], [11], [12], [13], [14], [15], [16], [17], [18], [19], [20], [21] ignored the effects of PLIs during RSA which might lead to the degraded quality-of-transmission (QoT) of lightpath

The associate editor coordinating the review of this manuscript and approving it for publication was Tianhua Xu.

signals in terms of bit error rate (BER) both in working and backup paths. On the other hand, few works [22], [23], [24], [25], [26], [27], [28], [29], [30], [31], [32] in literature addressed the problem of assuring minimum QoT for lightpath signals against PLIs but were implemented only for unprotected networks. This results in severe problems during the link/SRLG failures as mentioned before. Therefore, considering the practical scenarios, it is indispensable to design RSA in EON which protects the network against link/SRLG failures as well as ensures the minimum QoT for lightpath signals in both working and backup paths. Thus, in this paper, we design QoT guaranteed RSA in presence of PLIs in SBPP based EON against single link/SRLG failures.

It should be noted that, QoT assured SBPP EON cannot be designed easily by just combining existing studies related to SBPP EONs and QoT guaranteed unprotected EONs. The problem of ensuring QoT in survivable EON is fundamentally different and challenging than that of unprotected EONs due to the following reasons. In unprotected EONs, ensuring QoT guaranteed allocation for any request is the function of allocations of existing requests in the network as interference due to PLIs on any frequency slot (FS) depends on allocations. When it comes to survivable EONs, interference scenario is completely different. This is because, if we consider a particular link/SRLG failure in the network, working paths of existing requests containing the failed link/SRLG are deactivated and corresponding backup paths are activated. From this, we can observe that, set of requests whose working paths are active and the set of requests whose backup paths are active in the network varies with the failed link/SRLG. Therefore, different interference scenarios exist in survivable EON for different link/SRLG failures. Thus, unlike unprotected EONs, ensuring QoT guaranteed allocation for any request in survivable EONs is not only a function of allocations of existing requests but also a function of failed link/SRLG. Since we do not know which link/SRLG of the network will fail beforehand, allocation should be such that whichever link/SRLG fails QoT is guaranteed in all working and backup paths. For this purpose, we need to consider each possible allocation in the network corresponding to each single link/SRLG failure case before allocating any FS in working and backup path of each request. Considering above mentioned issues, we propose a *robust optimization* based RSA in this study wherein allocation of FS and its modulation format (MF) is carried out based on maximum possible interference (on particular FS) among all interferences corresponding to each single link/SRLG failure. Noteworthy, In the process of robust RSA design, we can also observe that each FS experiences different maximum possible (robust) interference considering each link/SRLG failure scenario. Therefore, each FS of a request can be assigned with different MF based on robust interference on that FS. This method of spectrum allocation can be termed as robust bitloading which offers extra challenges (compared to uniform modulation scheme) as the required number of FSs to accommodate the data rate requirement of a given request is unknown in advance.

TABLE 1. List of abbreviations.

ASE	amplified spontaneous emission
BBP	bandwidth blocking probability
BER	bit error rate
BS	broadcast and select
BVT	bandwidth variable transponder
EON	elastic optical network
FS	frequency slot
GN	Gaussian noise
ICC	inter-channel crosstalk
ICCI	ICC interference
IXT	in-band crosstalk
IXTI	IXT interference
LO	local oscillator
MCW-LCBF	most congested working-least congested backup first
MDF	most data rate first
MF	modulation format
MILP	mixed integer linear programming
PLI	physical layer impairment
QoT	quality-of-transmission
RSA	routing and spectrum allocation
SBPP	shared backup path protection
SBPP-IA	SBPP-impairment aware
SBPP-SWP	SBPP-spectrum window plane
SINR	signal to interference plus noise ratio
$SINR_{th}$	SINR threshold
SNR	signal to noise ratio
SRLG	shared risk link group
XC	cross-connect

The rest of the paper is organized as follows. Section II and III describe the state of the art and challenges, motivation, contributions of our problem respectively. Section IV, V and VII present the MILP formulation, the heuristic algorithm and the SRLG extension respectively. Section VIII provides simulation results for performance evaluation while Section IX concludes the paper.

II. RELATED WORK

In this section, we present the existing studies related to RSA design in SBPP based EON and QoT guaranteed unprotected EON. Under the static traffic scenario, Shen et al. [3] developed integer linear programming (ILP) models for both SBPP and 1 + 1 path protection based EONs to analyze and compare their performance. They also examined the impact of both transponder tunability and bandwidth squeezed restoration techniques. Authors in [4] presented a survivable hybrid protection lightpath (HybPL) algorithm to minimize spectrum utilization in the network. In this algorithm, resource availability and power consumption together decide whether to provide dedicated or shared path protection. In [5], authors focused on RSA design of survivable EON against dual link failures for various sharing capabilities of backup lightpaths. For this purpose, they developed ILP and heuristics with the goal of minimizing total number of FSs used. Cai et al. formulated mixed integer linear programming (MILP) and proposed a heuristic algorithm for routing, modulation level, and spectrum assignment (RMLSA) problem for multicast capable EON with shared protection [6]. Authors in [7] considered integrated multilayer protection problem in IP over EONs against single link or router failure

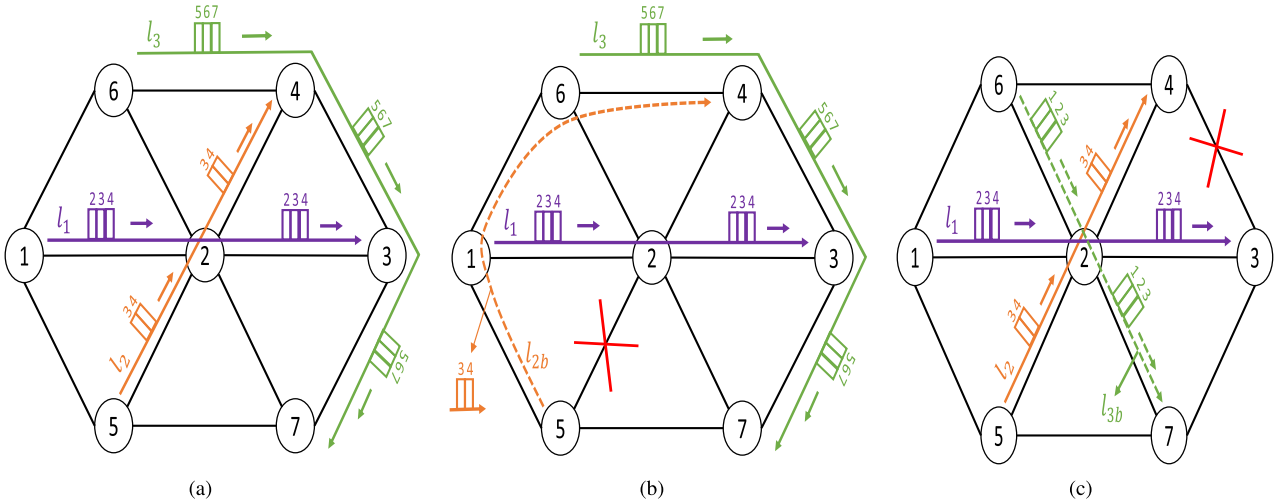

FIGURE 1. Effect of in-band crosstalk on FS '3' at XC '2' under different link failure conditions. (a) No link failure (b) 5-2 link failure (c) 4-3 link failure.

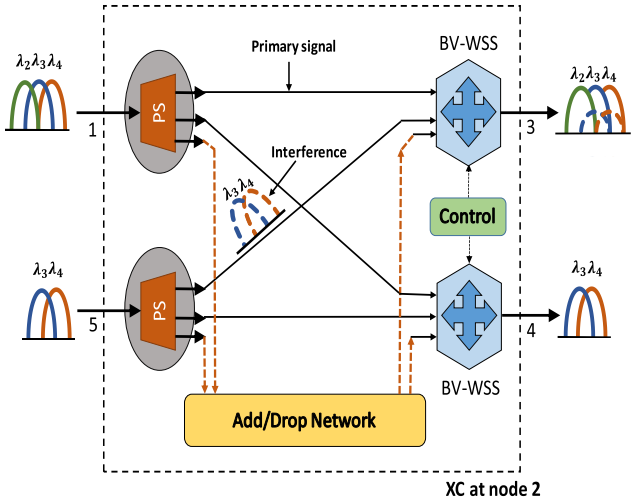

FIGURE 2. Formation of in-band crosstalk in cross-connect (XC) at node 2; PS: passive splitter; BV-WSS: bandwidth variable wavelength selective switch.

at any time. To address this problem, they presented an ILP model and proposed efficient algorithms. Various other works related to shared protection based EON under static traffic are presented in [8], [9], [10], [11], [12], [13], [14], and [15].

Considering the dynamic traffic scenario, authors in [16] presented minimum free spectrum-block consumption algorithm to solve the RSA problem for SBPP EON with the objective of reducing total spectrum usage while satisfying the joint failure probability threshold. Authors in [17] focused on distance adaptive RSA problem for EON with SBPP for which they proposed spectrum window plane based heuristic algorithms. Moreover, authors in this study considered differentiated shareable FS cost to share the backup FSs more efficiently. In addition, significant research has been carried out regarding dynamic SBPP EON in [18], [19], [20], [21]. However, all the above mentioned studies did not consider the effect of PLIs in RSA design of SBPP EON.

With respect to PLI aware studies, authors in [22], [23], [24], [25], [26], [27], [28], [29], [30], [31], and [32] considered various impairments such as in-band crosstalk, nonlinear impairments, filtering effects and amplified spontaneous emission noise etc. in RSA to ensure minimum QoT for all requests. But, the authors in these studies did not extend their work to design survivable EONs.

As mentioned in the introduction, existing works related to SBPP EON ignored the effect of PLIs in RSA design and the studies where PLIs were taken into account in RSA design did not consider the protection against link/SRLG failures. Therefore, it is imperative to design a robust RSA in EON to ensure both protection against link/SRLG failures as well as minimum QoT in working and backup paths against PLIs.

III. CHALLENGES, MOTIVATION AND CONTRIBUTIONS

In this section, we describe the challenges and motivation of our considered problem. In this regard, we discuss the concept of PLIs first.

A. PHYSICAL LAYER IMPAIRMENTS

PLIs such as shot noise, amplified spontaneous emission (ASE) noise, crosstalk (in-band and out-of-band), nonlinear impairments, filtering effects and beat noises due to coherent reception, etc., degrade the quality of lightpath signal and limit its optical reach [27]. Among these, in-band crosstalk (IXT) is severely coupled with the RSA framework [26]. Therefore, in this work, we target to ensure the minimum QoT for working and backup lightpath signals by considering the IXT as a major source of interference along with ASE and beating noise terms due to coherent reception. In general, the generation of IXT in any optical network is due to the non-ideal nature of the switch used in cross-connect (XC). When two or more lightpath signals co-propagate through

the same XC, subcarrier of each signal gets interference from the subcarriers of other signals having same frequency. This effect will be more if the signal propagates through multiple XCs in its path. We approximate IXT interference and the ASE noise independently using generalized Gaussian model [33], [34]. Further, we also assume that IXT interferences and ASE noise are additive as the corresponding devices which generate them are not nonlinear.

Now, we illustrate the challenges associated with IXT to ensure the minimum QoT in working and backup paths of each request in SBPP based EON with a suitable example.

B. CHALLENGES TO ENSURE QoT IN SBPP EON

We consider a 7-node network as shown in Fig. 1 in which each link is bi-directional. Each rectangular box in Fig. 1 denotes the FS or subcarrier that is being used by the request. A request r_i is described as $r_i(s, d)$ where, s and d stands for source and destination, respectively. We consider 3 requests $r_1(1, 3)$, $r_2(5, 4)$ and $r_3(6, 7)$. Provisioning of working paths for these 3 requests is shown in Fig. 1(a) represented by l_1,l_2 and l_3. Here, we analyze the effect of IXT on FS '3' in lightpath l_1 at XC '2' under different link failure conditions. For this purpose, first we assume that there is no failure in the network as shown in Fig. 1(a). In this case, FS '3' in l_1 experiences IXT interference (IXTI) from the FS '3' present in lightpath l_2 at XC '2' as shown in Fig. 2. Note that, λ_2,λ_3 and λ_4 shown in Fig. 2 denotes FS 2,3 and 4 respectively. Next, we consider that link 5-2 is failed as shown in Fig. 1(b). Due to this, working path l_2 of request r_2 is affected which is rerouted through the backup path denoted as l_{2b}. In this case, FS '3' in l_1 does not get interference from any other lightpaths at XC '2'. Similarly, for 4-3 link failure, working path l_3 of request r_3 is affected and switch over is carried out to its backup path l_{3b} as shown in Fig. 1(c). Here, FS '3' in l_1 gets interference at XC '2' from lightpaths l_2 and l_{3b} which are using FS '3'. From the above discussion, we made the following observations. Firstly, set of existing requests whose working paths are active (R_w) and the set of existing requests whose backup paths are active (R_b) in the network varies with the failed link. As a result, different allocations get activated in the network for different link failures. Due to this, FS '3' of lightpath l_1 at XC '2' experiences different interference power for different link failures. This scenario is same for each FS in every link at all XCs in the network. Now, to have a QoT guaranteed allocation, FS '3' can only be allocated to any request if and only if end-to-end signal to interference plus noise ratio (SINR) at FS '3' is greater than the required threshold (corresponding to targeted BER of 10^{-9}) of considered modulation format (MF). Since we do not know which link of the network will fail beforehand, we employ robust optimization based RSA wherein we calculate end to end interference at FS '3' by considering each link failure and obtain maximum value among them. As we are employing the maximum possible or robust interference (considering each link failure scenario) to calculate SINR (which gives robust SINR), QoT is guaranteed irrespective of the failed link. We follow the similar procedure before allocating each FS in working and backup path of every request. In addition, since robust interference and corresponding robust SINR is different for each FS, we can allocate different MF to each FS of a request based on robust SINR at that FS. Implementing this robust optimization based RSA through MILP and heuristic is a challenging task.

Considering the above challenges, we list our major contributions in this study as given below:

- We formulate a robust MILP optimization model in presence of IXTI along with ASE and beating noise terms for SBPP EON for benchmarking against single link failures.
- For realistic networks, we propose a novel robust optimization based heuristic for static and dynamic traffic.
- For the static heuristic, we propose novel probability of congestion based sorting technique which improves the shareability among backup FSs.
- In our optimization framework, we ensure minimum QoT guarantee in terms of BER for both working and backup paths under any single link failure and no link failure.
- We extend our MILP and heuristic to design QoT guaranteed RSA in SBPP EON against SRLG failures.
- We employ robust bitloading (assigning different MF for each FS of a request) technique for efficient spectrum allocation in our RSA design.
- For dynamic traffic scenario, we ensure the QoT of existing requests while accommodating each new request without reserving any margin. For this purpose, we again implement robust calculation of SINR on each FS of existing requests while allocating every FS of a new request.
- Through simulations, we demonstrate that RSA design in SBPP EON without considering PLIs contributes 33.94-41.02 percentage of QoT failed requests at 70 Tbps load whereas our design results in ''zero'' QoT failed requests without affecting blocking probability much.

IV. MILP FORMULATION

In this section, we provide the MILP design model for the problem discussed in previous section. In the formulation of MILP, we define our objective function and present the basic RSA constraints like spectrum continuity, contiguity and non overlapping constraints. In addition, we illustrate the backup spectrum sharing and other SBPP constraints in the design process. Further, we demonstrate how the minimum QoT is ensured in both working and backup paths under any single link failure and no link failure conditions through our MILP framework. Note that, we use the following assumptions through out our paper.

Assumptions: In this work, balanced heterodyne detection is considered for CO-OFDM system. In addition, we assume that primary and interfering lightpath signals have identical

power spectral density. We also consider that dispersion is perfectly compensated. Further, the bandwidth of each FS is assumed to be 12.5 GHz where we choose the base data rate with BPSK as 10 Gbps in each FS with 25% overhead. We also assume that each node consists of sufficient variable data rate modulators.

Note that, MILP input parameters and output variables are represented as [i/p] and [o/p], respectively. We use the following indices for the rest of our paper.

Indices

$r, r' \in R = \{1, 2, \ldots, C\}$	Set of given requests
$l, e \in L = \{1, 2, \ldots, E\}$	Set of links in the network
$f = \{1, 2, \ldots, N\}$	Available FSs in each link
$m = \{1, 2, \ldots, M\}$	Available MFs

Objective:

$$minimize \quad \sum_{l} \sum_{f} f \times H_{f,l} \tag{1}$$

The objective of our MILP is to minimize the sum of highest indexed FS used in each link of the network to minimize the fragmentation in all links. $H_{f,l}$ in (1) is set to 1 if FS *'f'* is the highest indexed allocated FS in link *'l'*, else 0.

Constraints:

Highest indexed allocated FS in each link *'l'* can be calculated by using the constraints (2-4). The parameters used in these constraints are described below

$\boldsymbol{H_{f,l}} = 1$ if FS *'f'* is the highest indexed allocated FS in link *'l'*, else 0. [o/p]

$\boldsymbol{X_{f,l}} = 1$ if FS *'f'* is allocated in link *'l'*, else 0. [o/p]

$$H_{f',l} \leq 1 - \frac{\sum_{f=f'+1}^{N} X_{f,l}}{N}; \ \forall l, \forall f' = \{1, \ldots, N-1\} \tag{2}$$

$$H_{f',l} \leq X_{f',l}; \quad \forall l, \forall f' = \{1, \ldots, N\} \tag{3}$$

$$\sum_{f'=1}^{N} H_{f',l} \geq \frac{\sum_{f'=1}^{N} X_{f',l}}{N}; \quad \forall l \tag{4}$$

1) WORKING AND BACKUP PATH SELECTION

For each request, we compute K shortest working paths and for each working path, we find K_b shortest backup paths (link disjoint to corresponding working path). The parameters required for these constraints are given below.

$\boldsymbol{P_r^w}$: Set of working paths of request *'r'*. [i/p]

$\boldsymbol{P_{r,p}^b}$: Set of backup paths of working path $p \in P_r^w$. [i/p]

$\boldsymbol{W_p^r} = 1$ if request *'r'* selects working path *'p'*, else 0. [o/p]

$\boldsymbol{B_{p_b,p}^r} = 1$ if request *'r'* chooses backup path 'p_b' of working path *'p'*, else 0. [o/p]

$$\sum_{p \in P_r^w} W_p^r = 1; \quad \forall r \tag{5}$$

$$\sum_{p_b \in P_{r,p}^b} B_{p_b,p}^r = W_p^r; \quad \forall p \in P_r^w, \forall r \tag{6}$$

Constraint (5) guarantees that each request *'r'* selects one working path *'p'* from set of its working paths. Next, constraint (6) ensures that each request *'r'* chooses one backup path 'p_b' from set of backup paths of selected working path *'p'*.

2) SPECTRUM AND MODULATION ASSIGNMENT

The parameters associated with these constraints are defined as follows:

$\boldsymbol{\rho^r}$: Integer, data rate demand of request *'r'*. [i/p]

$\boldsymbol{\Phi}$: Base data rate per FS with BPSK (10 Gbps in our case). [i/p]

$\boldsymbol{W_{m,f,p}^r} = 1$ if FS *'f'* with MF *'m'* is allocated in working path *'p'* of request *'r'*, else 0. [o/p]

$\boldsymbol{B_{m,f,p_b,p}^r} = 1$ if FS *'f'* with MF *'m'* is allocated in backup path 'p_b' of working path *'p'* of request *'r'*, else 0. [o/p]

$$W_p^r \times \rho^r = \sum_{m} \sum_{f} m.\Phi.W_{m,f,p}^r; \quad \forall p \in P_r^w, \forall r \tag{7}$$

$$B_{p_b,p}^r \times \rho^r = \sum_{m} \sum_{f} m.\Phi.B_{m,f,p_b,p}^r; \quad \begin{cases} \forall p_b \in P_{r,p}^b, \\ \forall p \in P_r^w, \forall r \end{cases} \tag{8}$$

Constraint (7) selects the FSs and corresponding MFs to be allocated in selected working path *'p'* to satisfy the data rate demand of request *'r'*. Noteworthy, MF of each FS is chosen based on the end-to-end SINR at that FS such that SINR at FS is greater than the SINR threshold (for targeted BER) of chosen MF using the constraint (38) as described in subsection IV-11. Further, as shown in constraint (7), MF chosen for each FS decides the number of required FSs for a particular request *'r'* to satisfy the data rate demand (ρ^r). Similarly, constraint (8) (with the help of constraint (39) in subsection IV-11) determines the FSs and corresponding MFs to be assigned in chosen backup path 'p_b' of selected working path *'p'* for request *'r'*. Note that, since we use robust bitloading technique in spectrum allocation, each FS can be allocated with different MF in working and backup path of each request.

$$\sum_{m} \sum_{p \in P_r^w} W_{m,f,p}^r \leq 1; \ \forall f, r \tag{9}$$

$$\sum_{m} \sum_{p \in P_r^w} \sum_{p_b \in P_{r,p}^b} B_{m,f,p_b,p}^r \leq 1; \ \forall f, r \tag{10}$$

Constraint (9) ensures that each selected FS is assigned with only one MF in one chosen working path *'p'* for each request *'r'*. Likewise, constraint (10) guarantees that only one MF is allocated for every chosen FS in one selected backup path 'p_b' of chosen working path *'p'* for each request *'r'*.

3) SPECTRUM CONTIGUITY CONSTRAINT

The following parameters are used in these constraints.

$\boldsymbol{\psi_{m,f,p}^r} = 1$ if there exists a transition from free FS '$f-1$' to FS 'f' that is allocated to request 'r' with MF 'm' in working path 'p', else 0. [o/p]

$\boldsymbol{\chi_{m,f,p_b,p}^r} = 1$ if there exists a transition from free FS '$f-1$' to FS 'f' that is allocated to request 'r' with MF 'm' in backup

path 'p_b' of working path 'p', else 0. [o/p]

$$\psi^r_{m,f,p} \geq \begin{cases} W^r_{m,f,p} - W^r_{m,f-1,p} & \text{if } f > 1 \\ W^r_{m,f,p} & \text{if } f = 1 \end{cases} \Big\{ \forall p \in P^w_r, \forall m, f, r \quad (11)$$

$$\sum_m \sum_f \sum_{p \in P^w_r} \psi^r_{m,f,p} = 1; \quad \forall r \quad (12)$$

$$\chi^r_{m,f,p_b,p} \geq \begin{cases} B^r_{m,f,p_b,p} - B^r_{m,f-1,p_b,p} & \text{if } f > 1 \\ B^r_{m,f,p_b,p} & \text{if } f = 1 \end{cases} \Big\{ \forall p_b \in P^b_{r,p}, \forall p \in P^w_r, \forall m, f, r \quad (13)$$

$$\sum_m \sum_f \sum_{p \in P^w_r} \sum_{p_b \in P^b_{r,p}} \chi^r_{m,f,p_b,p} = 1; \quad \forall r \quad (14)$$

Constraints (11), (12) and (13), (14) ensure the contiguity constraint of EON for working and backup path, respectively, of each request 'r'. If FS 'f' is chosen in path, then constraints (11)-(14) make sure that FSs $f+1, f+2$ and so on will be selected till the requested data rate is satisfied.

4) SPECTRUM NON-OVERLAPPING WORKING AND BACKUP PATHS

The parameters employed in these constraints are described in the following.

$\boldsymbol{\delta^r_{l,p}} = 1$ if working path 'p' of request 'r' contains the link 'l', else 0. [i/p]

$\boldsymbol{\delta^r_{l,p_b,p}} = 1$ if backup path 'p_b' of working path 'p' of request 'r' contains the link 'l', else 0. [i/p]

$\boldsymbol{W^r_{m,f,l}} = 1$ if FS 'f' with MF 'm' is allocated in link 'l' of the working path of request 'r', else 0. [o/p]

$\boldsymbol{B^r_{m,f,l}} = 1$ if FS 'f' with MF 'm' is allocated in link 'l' of the backup path of request 'r', else 0. [o/p]

$\boldsymbol{B_{f,l}} = 1$ if backup path of at least one request $r \in R$ is allocated with FS 'f' in link 'l', else 0. [o/p]

$\boldsymbol{X_{f,l}} = 1$ if FS 'f' is allocated in link 'l', else 0. [o/p]

$$\sum_{p \in P^w_r} W^r_{m,f,p} \times \delta^r_{l,p} = W^r_{m,f,l}; \quad \forall m, f, l, r \quad (15)$$

$$\sum_{p \in P^w_r} \sum_{p_b \in P^b_{r,p}} B^r_{m,f,p_b,p} \times \delta^r_{l,p_b,p} = B^r_{m,f,l}; \forall m, f, l, r \quad (16)$$

$$\frac{\sum_r \sum_m B^r_{m,f,l}}{N} \leq B_{f,l}; \forall f, l \quad (17)$$

$$\sum_r \sum_m W^r_{m,f,l} + B_{f,l} \leq X_{f,l}; \forall f, l \quad (18)$$

Constraints (17) and (18) enforce that working path of one request r and backup path of other request r' do not use the same FS(s) in their common links.

5) SPECTRUM NON-OVERLAPPING WORKING PATHS

Eq. (18) also ensures that working paths of two different requests do not use the same FS(s) in their common links.

6) BACKUP SHARING & LINK DISJOINT CONSTRAINT

Here in this MILP framework, we do not include the constraint for spectrum non-overlapping between backup paths of any two requests. This enables the sharing of spectrum resources among the backup paths. Further, since our objective function tries to do the allocation at left side of the spectrum, backup paths are allocated with maximum possible spectrum sharing. However, backup paths of requests can not share the spectrum unless their corresponding working paths are link disjoint. Therefore, we provide the link disjoint constraints in (19) and (20). Parameter $t^{r,r'}$ in (19) gives the value 1 if two different requests r and r' has at least one common link in their working paths, else 0. Then Eq. (20) ensures that spectrum sharing among the backup paths is possible only when their corresponding working paths are link disjoint.

$$t^{r,r'} \geq \frac{\sum_{m,m'=1}^{M} \sum_{f,f'=1}^{N} \sum_l W^r_{m,f,l} \times W^{r'}_{m',f',l}}{N};$$

$$t^{r,r'} \leq \sum_{m,m'=1}^{M} \sum_{f,f'=1}^{N} \sum_l W^r_{m,f,l} \times W^{r'}_{m',f',l}; \Big\{ \forall r, r' \text{ where, } r \neq r' \quad (19)$$

$$\sum_{m=1}^{M} B^r_{m,f,l} + \sum_{m'=1}^{M} B^{r'}_{m',f,l} \leq (2 - t^{r,r'}).X_{f,l}; \quad \forall f, l, r, r' \text{ where, } r \neq r' \quad (20)$$

7) SPECTRUM CONTINUITY CONSTRAINT

Constraints (7), (8), (9), (10), (15), (16), (17) and (18) also ensure that same FSs are allocated in all links of each working and backup path.

8) SINGLE LINK FAILURE CONSTRAINT

Constraint (21) fails a single link 'e' in the network if there is a failure. Further, constraint (22) denotes the failed requests due to the failure of link 'e'.

$\boldsymbol{F_e} = 1$ if link 'e' is failed in the network, else 0. [o/p]

$\boldsymbol{F^r_{e,p}} = 1$ if failed link 'e' is present in working path 'p' of request 'r', else 0. [o/p]

$\boldsymbol{\delta^r_{e,p}} = 1$ if working path 'p' of request 'r' contains the link 'e', else 0. [i/p]

$$\sum_{e \in L} F_e = 1; \quad (21)$$

$$F_e \times \delta^r_{e,p} = F^r_{e,p}; \ \forall p \in P^w_r, \forall e \in L, \forall r \quad (22)$$

As mentioned before, each FS in working and backup path of every request experiences different IXTI effect for different single link failures and no link failure conditions due to the presence of different active working and backup paths. Since we do not know which link of the network will fail beforehand, robust optimization based RSA is required to ensure the QoT under any link failure scenario. For this purpose, we calculate the end-to-end interference at FSs in working

and backup path of every request due to the active working and backup paths of other requests considering a particular link failure. We repeat the above procedure for each single link failure case and no link failure case and calculate the maximum possible (robust) end-to-end interference among the above mentioned scenarios at FSs in working and backup path of every request. Now, the allocation is carried out based on robust interference value at each FS of every request. Since we are employing robust interference (considering each link failure scenario), whichever link fails, QoT is guaranteed in working and backup paths of each request. Above procedure is implemented using following constraints.

9) MAXIMUM POSSIBLE (ROBUST) CROSSTALK INTERFERENCE CALCULATION IN WORKING PATHS

Crosstalk interference power generated at FS *'f'* with MF *'m'* in link *'l'* of targeted working path *'p'* of request *'r'* for the failure of link *'e'* ($l \neq e$) is equal to the sum of all crosstalk powers due to FS *'f'* used in active working and backup paths of other requests which are passing through the head node of link *'l'* (denoted by *'i'*) as shown in (23). This computation is done for all FSs in each link of all working paths of all requests by considering each link failure *'e'* in the network except the links present in targeted working path.

$$\begin{aligned}\mathrm{Pxt}^{w,r}_{m,f,p,l,e} &= \sum_{r'\in R/r}\sum_{p'\in P^{w}_{r'}}\sum_{m'=1}^{M}\sum_{j'=1}^{N}\Big[P^{r'}_{m',f,p',j',i}.W^{r'}_{m',f,p'}.(1-F^{r'}_{e,p'}) \\ &\quad + \sum_{p'_b\in P^{b}_{r',p'}} P^{r'}_{m',f,p'_b,p',j',i}.B^{r'}_{m',f,p'_b,p'}.F^{r'}_{e,p'}\Big]; \\ &\quad \Big\{\forall e\in L/l_p, \forall l\in l_p, \forall p\in P^{w}_{r}, \forall m,f,r \quad (23)\end{aligned}$$

Here, l_p denotes the set of links present in working path *'p'* and $P^{r'}_{m',f,p',j',i}$ is the power of interfering signal added at node *'i'* (head node of link *'l'*) which is using FS *'f'* with MF m' and traverses from the node j' to the XC present in node *'i'*, where j'-i is the link present in working path p' of request r'. Next, the definition of $P^{r'}_{m',f,p'_b,p',j',i}$ in Eq. (23) is same as $P^{r'}_{m',f,p',j',i}$ except that j'-i is the link present in backup path p'_b of working path p' of request r'. $P^{r'}_{m',f,p',j',i}$ and $P^{r'}_{m',f,p'_b,p',j',i}$ are calculated as given below.

$$P^{r'}_{m',f,p',j',i} = P^{r'}_{m',f,p'_b,p',j',i} = P_r \times C_x \quad (24)$$

where, P_r denotes the received signal power (we assume equal power for each FS) and C_x represents the crosstalk factor of the switch. Note that, $P^{r'}_{m',f,p',j',i} = 0$ if no link exists between the nodes j' and i in working path p' and $P^{r'}_{m',f,p'_b,p',j',i} = 0$ if there is no link between j' and i in backup path p'_b of working path p'.

Further, total aggregated crosstalk interference power at FS *'f'* with MF *'m'* at the destination node of targeted working path *'p'* of request *'r'* for the failure of link *'e'* is computed by adding the crosstalk power at FS *'f'* in each link of the path *'p'* for the failure of link *'e'* as shown in (25). The above calculation is repeated for the failure of each link *'e'* in the network except the links present in targeted path *'p'*. Next, the whole process is repeated for all FSs in each working path of every request.

$$\mathrm{Pxt}^{w,r}_{m,f,p,e} = \sum_{l\in l_p}\mathrm{Pxt}^{w,r}_{m,f,p,l,e}; \begin{cases}\forall e\in L/l_p, \forall p\in P^{w}_{r},\\ \forall m,f,r\end{cases} \quad (25)$$

Note that, $\mathrm{Pxt}^{w,r}_{m,f,p,e}$ in constraint (25) is different for different link failures due to the existence of different active working and backup paths. Therefore, maximum among all crosstalk power values that $\mathrm{Pxt}^{w,r}_{m,f,p,e}$ constitutes considering each link failure *'e'* is calculated as given in (26). This process is repeated for all FSs in each working path of every request.

$$\mathrm{Pxt}^{w,r,max_e}_{m,f,p} = \max_{e\in L/l_p}\left\{\mathrm{Pxt}^{w,r}_{m,f,p,e}\right\}; \forall p\in P^{w}_{r}, \forall m,f,r \quad (26)$$

Further, we also enumerate the crosstalk interference power at all FSs of each working path of all requests under no link failure using the constraints (27-28).

$$\begin{aligned}\mathrm{Pxt}^{w,r}_{m,f,p,l} &= \sum_{r'\in R/r}\sum_{p'\in P^{w}_{r'}}\sum_{m'=1}^{M}\sum_{j'=1}^{N}\left[P^{r'}_{m',f,p',j',i}.W^{r'}_{m',f,p'}\right]; \\ &\quad \Big\{\forall l\in l_p, \forall p\in P^{w}_{r}, \forall m,f,r \quad (27)\end{aligned}$$

$$\mathrm{Pxt}^{w,r}_{m,f,p} = \sum_{l\in l_p}\mathrm{Pxt}^{w,r}_{m,f,p,l};\ \forall p\in P^{w}_{r}, \forall m,f,r \quad (28)$$

Finally, maximum possible crosstalk power at each FS *'f'* with MF *'m'* at the destination node of every working path *'p'* of each request *'r'* considering all possible single link failure and no link failure conditions is computed as shown in (29).

$$\begin{aligned}\mathrm{Pxt}^{w,r,max}_{m,f,p} &= \max\left\{\mathrm{Pxt}^{w,r,max_e}_{m,f,p}, \mathrm{Pxt}^{w,r}_{m,f,p}\right\}; \\ &\quad \Big\{\forall p\in P^{w}_{r}, \forall m,f,r \quad (29)\end{aligned}$$

From Eqs. (23)-(29), we can observe that, maximum possible (robust) end-to-end crosstalk interference calculated in (29) is different for each FS of a particular request. Therefore, in this MILP formulation, we employ robust bitloading where each FS of a request is assigned with different MF (in both working and backup paths) based on robust SINR at that FS using Eqs.(38) and (39).

10) MAXIMUM POSSIBLE (ROBUST) CROSSTALK INTERFERENCE CALCULATION IN BACKUP PATHS

By following the similar approach used for working path, we calculate the maximum possible crosstalk interference power at each FS in every backup path of all requests using the constraints (30-32). Note that, unlike for working paths, while finding maximum possible interference for backup paths, we fail one link of its working path as backup path is enabled when its working path fails. Next, the definitions of parameters used in these constraints are same as that we

used for working paths in previous subsection. By replacing *'w'* with *'b'* and '*p*' (working path) with p_b, p (backup path 'p_b' of working path 'p') in the parameters used in previous section, we get the required description for the parameters used in these constraints.

$$\begin{aligned}&\mathrm{Pxt}^{b,r}_{m,f,p_b,p,l,e}\\&= \sum_{r'\in R/r}\sum_{p'\in P^w_{r'}}\sum_{m'=1}^{M}\sum_{j'=1}^{N}\Big[P^{r'}_{m',f,p',j',i}.W^{r'}_{m',f,p'}.(1-F^{r'}_{e,p'})\\&\quad+\sum_{p'_b\in P^b_{r',p'}}P^{r'}_{m',f,p'_b,p',j',i}.B^{r'}_{m',f,p'_b,p'}.F^{r'}_{e,p'}\Big];\\&\qquad\Big\{\forall e\in l_p,\forall l\in l_{p_b,p},\forall p_b\in P^b_{r,p},\forall p\in P^w_r,\forall m,f,r\end{aligned}\tag{30}$$

$$\begin{aligned}&\mathrm{Pxt}^{b,r}_{m,f,p_b,p,e}\\&=\sum_{l\in l_{p_b,p}}\mathrm{Pxt}^{b,r}_{m,f,p_b,p,l,e};\\&\qquad\Big\{\forall e\in l_p,\ \forall p_b\in P^b_{r,p},\forall p\in P^w_r,\forall m,f,r\end{aligned}\tag{31}$$

$$\begin{aligned}&\mathrm{Pxt}^{b,r,max}_{m,f,p_b,p}\\&=\max_{e\in l_p}\Big\{\mathrm{Pxt}^{b,r}_{m,f,p_b,p,e}\Big\};\\&\qquad\Big\{\forall p_b\in P^b_{r,p},\forall p\in P^w_r,\forall m,f,r\end{aligned}\tag{32}$$

11) QoT GUARANTEE CONSTRAINTS

The necessary parameters for these constraints are introduced in the following.

$\boldsymbol{P_{ch}}$: Coherently received power at any FS. [i/p]

$\boldsymbol{SNR^r_{f,p}}$: Signal to noise ratio (SNR) at FS *'f'* in working path *'p'* of request *'r'*. [i/p]

$\boldsymbol{\sigma^{2|(r,p)}_{lo-sp}}$: Local oscillator (LO)-ASE beat noise variance in working path *'p'* of request *'r'*. [i/p]

$\boldsymbol{\zeta}$: $(R_a^2/2)P_{lo}2\eta_{sp}hf_cB_e$ (refer Table 2 for each term). [i/p]

$\boldsymbol{M^r_p}$: Number of EDFAs required in working path *'p'* of request *'r'*. [i/p]

$\boldsymbol{E_s}$: EDFA spacing. [i/p]

$\boldsymbol{\sigma^{2|(w,r,m,f,p,max)}_{lo-x}}$: Maximum possible local oscillator (LO)-crosstalk beat noise variance at FS *'f'* using MF *'m'* in working path *'p'* of request *'r'*. [o/p]

$\boldsymbol{IST^w_m}$: Denotes value of inverse of signal-to-interference-plus-noise-ratio (SINR) threshold for selected working path for MF *'m'* (refer [27] for BER expression). [i/p]

$\boldsymbol{LN}$: Large number $\gg IST^w_M$; where, M is the maximum available MF. [i/p]

Parameters related to working path *'p'* are described above. By replacing *'w'* with *'b'* and '*p*' (working path) with p_b, p (backup path 'p_b' of working path 'p') in above parameters and corresponding description, we get the required parameters and description for the backup paths as well.

To ensure minimum QoT guaranteed allocation, any FS is allocated in either working or backup path if and only if end-to-end SINR at that FS is greater than or equal to SINR threshold ($SINR_{th}$) of considered MF. Therefore,

$$\begin{aligned}SINR\geq SINR_{th}\ &\Longrightarrow\ P_{ch}/(P_I+P_N)\geq SINR_{th}\\&\Longrightarrow\ \frac{P_I}{P_{ch}}+\frac{1}{SNR}\leq\frac{1}{SINR_{th}};\end{aligned}\tag{33}$$

where, *Pch*: Coherently received signal power; P_I: Interference power; P_N: Noise power. Eq. (33) is the underlying equation for QoT guarantee constraints of (38) and (39).

The combined noise term includes LO-crosstalk (P_I) and LO-ASE (P_N) beat noises when the system is assumed to be operated well above the shot noise limit with high LO power (refer [26] for a complete analysis). Next, Each term in (33) is calculated as follows:

$$SNR^r_{f,p}=\frac{P_{ch}}{\sigma^{2|(r,p)}_{lo-sp}},\ \text{where, } P_{ch}=(R_a^2/2)P_{lo}P_r,\tag{34}$$

$$\sigma^{2|(r,p)}_{lo-sp}=\zeta\left(M^r_p(G_{in}-1)+\sum_{i=1}^{Z-1}(G_{out}(i)-1)\right)\tag{35}$$

where, $M^r_p=\frac{\sum_{l\in l_p}\triangle_l}{E_s}$; $\triangle_l$: link distance

In Eq. (35), G_{in} denotes the input EDFA gain and $G_{out}(i)$ represents the output EDFA gain at node $i=1,2,\ldots,Z$ in working path 'p' of request *'r'* and given as [27], $G_{out}(i)\geq 3\lceil log_2Q(i)\rceil+L_{WSS}$ dB, where $Q(i)$ is the fiber inputs/outputs at node 'i'. Each parameter in Eq. (35) is related to broadcast and select node architecture presented in [27] which is employed for this work as well.

Similarly, $SNR^r_{f,p_b,p}$ and $\sigma^{2|(r,p_b,p)}_{lo-sp}$ are computed by replacing 'p' (working path) with p_b, p (backup path 'p_b' of working path 'p') in (34) and (35), respectively. Further, LO-crosstalk beat noise terms for working and backup paths are enumerated as given in (36) and (37), respectively.

$$\sigma^{2|(w,r,m,f,p,max)}_{lo-x}=(R_a^2/2)P_{lo}\mathrm{Pxt}^{w,r,max}_{m,f,p}\tag{36}$$

$$\sigma^{2|(b,r,m,f,p_b,p,max)}_{lo-x}=(R_a^2/2)P_{lo}\mathrm{Pxt}^{b,r,max}_{m,f,p_b,p}\tag{37}$$

where, $\mathrm{Pxt}^{w,r,max}_{m,f,p}$ and $\mathrm{Pxt}^{b,r,max}_{m,f,p_b,p}$ are from (29) and (32), respectively.

Now, QoT guarantee constraints for working and backup paths are formulated as shown in (38) and (39), respectively.

$$\begin{aligned}&\frac{\sigma^{2|(w,r,m,f,p,max)}_{lo-x}}{P_{ch}}+\frac{W^r_{m,f,p}}{SNR^r_{f,p}}+LN\times W^r_{m,f,p}\\&\quad\leq LN+IST^w_m;\ \Big\{\forall p\in P^w_r,\forall m,f,r\end{aligned}\tag{38}$$

$$\begin{aligned}&\frac{\sigma^{2|(b,r,m,f,p_b,p,max)}_{lo-x}}{P_{ch}}+\frac{B^r_{m,f,p_b,p}}{SNR^r_{f,p_b,p}}+LN\times B^r_{m,f,p_b,p}\\&\quad\leq LN+IST^b_m;\ \Big\{\forall p_b\in P^b_{r,p},\forall p\in P^w_r,\forall m,f,r\end{aligned}\tag{39}$$

With respect to working path, when a particular $W^r_{m,f,p}=1$, then Eq. (38) is similar to (33). On the other hand, when $W^r_{m,f,p}=0$, then *LN* makes sure that Eq. (38) is valid. Above description also holds for backup path QoT guarantee constraint given in (39). Thus, constraint (38)

(or 39) ensures that, any FS with some MF is allocated in the working (or backup) path only when the robust end-to-end SINR at respective FS satisfies the SINR threshold criterion of the considered MF. Note that, robust end-to-end SINR at any FS in working (or backup) path corresponds to maximum possible (robust) interference at that FS which is calculated in subsections IV-9 and IV-10, respectively. Since we considered robust interference (considering each link failure scenario), minimum QoT assured allocation is guaranteed in both working and backup paths under any single link failure and no link failure conditions.

It is worth mentioning that, Equations (38) and (39) which gets reflected to (29) and (32) via (36) and (37) consists a maximization problem over interference powers corresponding to each link failure which is a random event. This makes our problem a *robust optimization problem* which contains maximization in the constraints and minimization in the objective. Therefore, our problem is not a regular ILP to solve and has to be converted to normal ILP by changing maximization constraint into linear as shown in the appendix.

Noteworthy, nonlinear constraints formulated in our MILP (Eqs. (19), (20), (23), (26), (29), (30), (32)) are converted into linear by following the standard procedure shown in appendix.

V. HEURISTIC ALGORITHM

It is proven that RSA without impairments in EON is NP-Hard problem [35]. The computational complexity of our proposed MILP increases exponentially with size and traffic of the network. In view of this, we propose a near optimal heuristic algorithm for realistic large network topologies. In this section, we propose a novel sorting technique to order the given static traffic requests followed by a heuristic algorithm to solve our problem under static and dynamic traffic scenarios. Note that, indices and parameters used in MILP are also employed in this section.

A. SORTING OF REQUESTS FOR STATIC TRAFFIC

It is worth mentioning that, sorting the requests is an integral part of any heuristic design for static traffic scenario as it influences the performance of heuristic in terms of optimality gap (G). *'G'* is the percentage deviation between MILP objective value and that of heuristic. Therefore, sorting technique should be such that the value of *'G'* is as minimum as possible. Note that, existing techniques sort the requests without taking the network congestion into account and there were no techniques so far which improves the shareability among backup FSs which results in high 'G' value. Therefore, in this work we propose a novel sorting technique named most congested working-least congested backup first (MCW-LCBF). In this technique we calculate the probability of congestion in each working and backup path of every request from each working and backup path of other requests. Since more congestion is disadvantageous for working path allocation and advantageous for backup path allocation, we sort the requests in such a way that more sharing of FSs among backup paths takes place. We describe the proposed sorting technique with the help of following steps.

Algorithm 1 MCW-LCBF Sorting Technique

```
for each request 'r' do
    Find K shortest working paths and for each working
      path, calculate K_b backup paths (link disjoint to
      corresponding working path) using Dijkstra's
      algorithm
    for each working path p do
        Calculate probability of congestion con_r^p using
          the Steps 2 and 3.
        for each backup path p_b do
            Compute probability of congestion con_r^{p_b,p}
              using the Steps 4 and 5
        end for
    end for
    Calculate average probability of congestion for
      request 'r' as con_r using Step 7
end for
Sort the requests in the descending order of their con_r
```

1) MCW-LCBF SORTING TECHNIQUE

Required parameters for the proposed sorting technique are as follows:

$\boldsymbol{l_p}$: Set of links present in working path 'p'.

$\boldsymbol{l_{p_b,p}}$: Set of links present in backup path 'p_b' of working path 'p'.

$\boldsymbol{x^{l,p,r}_{w_{p'},r'}}$: Probability that the link *'l'* of working path *'p'* of request *'r'* gets congestion from working path p' of request r', where, $r, r' \in R$ and $r \neq r'$.

$\boldsymbol{x^{l,p,r}_{b_{p'},r'}}$: Probability that the link *'l'* of working path *'p'* of request *'r'* gets congestion from backup paths of working path p' of request r', where, $r, r' \in R$ and $r \neq r'$.

$\boldsymbol{x^{l,p,r}_{r'}}$: Probability that the link *'l'* of working path *'p'* of request *'r'* gets congestion from working and backup paths of request r', where, $r, r' \in R$ and $r \neq r'$.

Step 1: For each request ($r \in R$), we find K shortest working paths and for each working path, we obtain K_b shortest backup paths (link disjoint to corresponding working path).

Step 2: Probability of congestion in each link present in every working path of each request ($r \in R$) from all other requests ($r' \in R/r$) is evaluated as follows:

If link *'l'* of working path *'p'* of request *'r'* goes through the working path p' of request r', then *'l'* gets congestion from p' if and only if request r' selects p' as its working path with probability $1/K$ as there are K working paths for r'. Therefore,

$$x^{l,p,r}_{w_{p'},r'} = \begin{cases} \frac{1}{K} & \text{if link 'l' of working path 'p' of request 'r'} \\ & \text{is present in working path } p' \text{ of request } r' \\ & \text{where, } r \neq r' \text{ and } p' \in P^w_{r'} \\ 0 & \text{otherwise} \end{cases} \tag{40}$$

Next, if link *'l'* of working path *'p'* of request *'r'* goes through any one of the backup paths of working path p' of request r', then *'l'* gets congestion from that backup path if r' selects it as its backup path. For this, first, r' has to select working path p' with probability $1/K$ and then choose one among K_b backup paths with probability $1/K_b$. Therefore, the total probability is $(1/K) * (1/K_b)$. If *'l'* goes through $D^l_{p'}$ number of backup paths of p' of r', probability will be $(1/K * 1/K_b * D^l_{p'})$ as in (41).

$$x^{l,p,r}_{b_{p'},r'} = \frac{1}{K} * \frac{1}{K_b} * D^l_{p'}\,;\ \text{where, } D^l_{p'} \text{ denotes the number of backup paths (contains the link } 'l' \text{ of working path } 'p' \text{ of request } 'r') \text{ of working path } p' \text{ of request } r', \text{ where, } r \neq r' \text{ and } p' \in P^w_{r'} \tag{41}$$

Sum of the probabilities in (40) and (41) over all working paths p' of request r' gives the total probability that link *'l'* of working path *'p'* of request *'r'* gets congestion from r' as given in (42).

$$x^{l,p,r}_{r'} = \sum_{p' \in P^w_{r'}} (x^{l,p,r}_{w_{p'},r'} + x^{l,p,r}_{b_{p'},r'})\,; \tag{42}$$

Now, the probability of congestion at any FS *'f'* (CSL) in link *'l'* of working path *'p'* of request *'r'* from all other requests $r' \in R/r$ is given as

$$CSL^{l,p}_r = \sum_{r' \in R/r} \frac{x^{l,p,r}_{r'} * \rho^{BPSK}_{r'}}{N}\,; \tag{43}$$

$\rho^{BPSK}_{r'}$ used in above equation represents the number of FSs required for requested data rate of each request ($\rho_{r'}$) when BPSK modulation is used for each FS. This means, we are considering the FSs allocation with uniform modulation using BPSK to consider the worst case scenario.

Finally, probability of congestion in link *'l'* of working path *'p'* of request *'r'* from all other requests $r' \in R/r$ is computed as

$$con^{l,p}_r = CSL^{l,p}_r * \rho^{BPSK}_r\,; \forall l \in l_p, \forall p \in P^w_r, \forall r \tag{44}$$

Step 3: Given the probability of congestion in each link of every working path, probability of congestion in each working path of every request is computed as shown below.

$$con^p_r = 1 - \prod_{l \in l_p} (1 - con^{l,p}_r)\,; \forall p \in P^w_r, \forall r \tag{45}$$

Step 4: By following similar approach in (43) and (44), we calculate the probability of congestion in each link present in every backup path of each working path of all requests.

$$CSL^{l,p_b,p}_r = \sum_{r' \in R/r} \frac{x^{l,p_b,p,r}_{r'} * \rho^{BPSK}_{r'}}{N}\,; \tag{46}$$

$$con^{l,p_b,p}_r = CSL^{l,p_b,p}_r * \rho^{BPSK}_r\,; \begin{cases} \forall l \in l_{p_b,p}, \forall p_b \in P^b_{r,p}, \\ \forall p \in P^w_r, \forall r \end{cases} \tag{47}$$

$x^{l,p_b,p,r}_{r'}$ is calculated using (40), (41) and (42) by replacing 'p' (working path) with p_b, p (backup path 'p_b' of working path 'p').

Step 5: Probability of congestion in each backup path of every working path of all requests is evaluated.

$$con^{p_b,p}_r = 1 - \prod_{l \in l_{p_b,p}} (1 - con^{l,p_b,p}_r)\,; \quad \forall p_b \in P^b_{r,p}, \forall p \in P^w_r, \forall r \tag{48}$$

Step 6: In general, from working path point of view, requests with more congestion in their working path should be allocated first as highly congested requests might not get enough resources if we don't allocate them first. Conversely, from backup path point of view, requests with less congestion in their backup path should be allocated first. This is because, since we ensure the sharing of spectrum in backup path, the lightly congested request has less chances of sharing the spectrum with other requests and thus difficult to get the resources if we allocate at the end. Therefore, to have a unified parameter for sorting, in this step, we calculate the ratios of individual working path's congestion to each of its corresponding backup path's congestion for every request.

$$\frac{con^p_r}{con^{p_b,p}_r}\,; \forall p_b \in P^b_{r,p}, \forall p \in P^w_r, \forall r \tag{49}$$

Step 7: We compute the average value of corresponding ratios of each request to find out the average probability of congestion for every request.

$$con_r = \frac{1}{(K * K_b)} \left[\sum_{p \in P^w_r} \sum_{p_b \in P^b_{r,p}} \frac{con^p_r}{con^{p_b,p}_r} \right]\,; \forall r \tag{50}$$

Step 8: Requests are sorted in descending order of their average probability of congestion evaluated in (50).

B. PROPOSED SBPP-IMPAIRMENT AWARE (SBPP-IA) ALGORITHM

Requests are allocated one by one in a sequence given by the proposed sorting technique in previous subsection. We execute the following steps to establish each request. Since we employ robust bitloading technique for spectrum allocation wherein each FS of a request can be allocated with different MF, number of FSs required to satisfy the data rate demand (ρ_r) of a given request *'r'* is unknown beforehand. Therefore, first we calculate the minimum number of FSs required (n_s) to establish *'r'* using the equation $n_s = \left\lceil \frac{\rho_r}{\Phi * M} \right\rceil$ (line 4, Algorithm 2), where, M is the spectrum efficiency of highest available MF, Φ denotes the base data rate per FS with BPSK (10 Gbps in our case).

1) ALLOCATION FOR WORKING PATH

For the allocation of working path, Algorithm 3 is called to implement the following steps (line 6, Algorithm 2). First we obtain an array CFS^p_r in which each element denotes the FS

Algorithm 2 SBPP-IA Heuristic Algorithm

1 Sort all the requests according to MCW-LCBF
2 **for** *each request 'r'* **do**
3 Find K shortest working paths and for each working path, calculate K_b backup paths (link disjoint to corresponding working path) using Dijkstra's algorithm
4 Calculate $n_s = \lceil \frac{\rho_r}{\Phi * M} \rceil$;
5 **for** *each working path p* **do**
6 Y=Working (ρ_r, n_s, p, r)
7 $AFS \leftarrow Y$
8 **for** *each backup path* p_b **do**
9 Y=Backup (ρ_r, n_s, p, p_b, r)
10 $AFS_b \leftarrow Y$
11 Calculate $obj_{p,r}^{p_b}$ by considering allocations in existing requests and AFS,AFS_b of current request
12 **end for**
13 **end for**
14 $obj(r) = \min_{p,p_b} \left(obj_{p,r}^{p_b}\right)$
15 Choose 'p' and 'p_b' combination for which $obj_{p,r}^{p_b}$ is minimum and allocate assigned FSs with MFs
16 **end for**

number from where n_s contiguous free FSs are present in considered working path *'p'* of request *'r'* (line 1, Algorithm 3). Note that, elements in CFS_r^p are sorted in ascending order using First-Fit algorithm [36] to minimize the fragmentation in each link of every working path of all requests. Now, we begin with first FS *'f'* in first set of n_s contiguous free FSs in path *'p'* (line 4, Algorithm 3). Next, we calculate the minimum possible or robust end-to-end SINR (considering each link failure) at targeted FS *'f'* in path *'p'* and we also compute the robust end-to-end SINR at *'f'* in working (p') and backup path (p'_b) of existing requests (R_{exi}) considering the allocation of targeted FS *'f'* in path *'p'* (lines 5-15, Algorithm 3). If robust SINR at *'f'* in p', p'_b of each request in R_{exi} satisfies the SINR thresholds of assigned MFs, we tentatively allocate FS *'f'* with the highest available MF *'m'* for which robust SINR at *'f'* in path *'p'* is greater than the SINR threshold of *'m'* (lines 16-21, 28-29 Algorithm 3). After the allocation of *'f'*, if data rate demand of request *'r'* is not satisfied, we go for next contiguous FS and repeat the same procedure for this new FS if it is free (lines 21,25, Algorithm 3). Conversely, if this new FS is not free, we discard the previous allocations and start with next set of n_s contiguous free FSs with fresh ρ_r (line 23, Algorithm 3) and repeat the above steps. If robust SINR at *'f'* in p', p'_b of any existing request fails to satisfy required thresholds of assigned MFs or if robust SINR at *'f'* in path *'p'* is less than the SINR thresholds of all available MFs, we discard the previous allocations and start with next set of n_s contiguous free FSs with fresh ρ_r (lines 32,35, Algorithm 3). The whole process is repeated till the requested data rate is allocated in path *'p'*.

Algorithm 3 Working (ρ_r, n_s, p, r)

1 Obtain CFS_r^p
2 $Y \leftarrow$ Empty array, $i = 1$
3 $\rho'_r = \rho_r$
4 $f = CFS_r^p(i)$
5 **for** *failure of each link (except the links in 'p')* **do**
6 **for** *each link 'l' present in path 'p'* **do**
7 Calculate in-band crosstalk interference (IXTI) at *'f'* in 'l' using (23)
8 **end for**
9 Calculate end-to-end IXTI at *'f'* in path 'p' by summing IXTIs calculated in each 'l' in line 7
10 **end for**
11 Calculate end-to-end IXTI at *'f'* in 'p' in no link failure case using (27) and (28)
12 Calculate maximum possible or robust end-to-end IXTI (maximum of all IXTIs calculated in lines 9 and 11) at *'f'* considering each link failure and no failure scenario
13 Calculate maximum possible or robust end-to-end IXTI at *'f'* in working (p') and backup path (p'_b) of existing requests (R_{exi}) considering the allocation of *'f'* in *'p'*
14 Calculate ASE noise in *'p'* of 'r' and in p', p'_b of R_{exi}
15 Compute minimum possible or robust end-to-end SINR (corresponding to maximum possible or robust IXTI) at *'f'* in *'p'* of 'r' and at *'f'* in p', p'_b of R_{exi}
16 **if** *robust SINR at 'f' in* p', p'_b *of each request in* R_{exi} *is greater than or equal to SINR threshold (to satisfy minimum QoT) of MFs assigned to them* **then**
17 Select highest available MF *'m'* for which robust SINR at *'f'* in *'p'* is greater than or equal to SINR threshold of *'m'*
18 **if** *any MF 'm' is available* **then**
19 $\rho'_r = \rho'_r - 10 * m$
20 **if** $\rho'_r > 0$ **then**
21 assign MF *'m'* to FS *'f'* and store *'f'* in the array $Y, f = f + 1$
22 **if** *new FS 'f' is not free* **then**
23 deallocate all allocated FSs in path *'p'*, empty the array Y, $i = i + 1$, goto line 3
24 **else**
25 goto line 5
26 **end if**
27 **end if**
28 **if** $\rho'_r = 0$ **then**
29 assign MF *'m'* to FS *'f'*, store *'f'* in Y, Return Y
30 **end if**
31 **else**
32 Empty the array Y, $i = i + 1$, goto line 3
33 **end if**
34 **else**
35 Empty the array Y, $i = i + 1$, goto line 3
36 **end if**

Algorithm 4 Backup (ρ_r, n_s, p, p_b, r)

1 Repeat the Algorithm 3 with the following changes.
   (a) Replace 'p' (working path) with p_b, p (backup path 'p_b' of working path 'p').
   (b) $CFS_r^{p_b,p}$ is obtained in such a way that sharing of FSs among backup paths occur subject to link disjoint constraint presented in subsection IV-6.
   (c) While finding maximum possible interference at targeted FS 'f' in considered backup path to ensure minimum end-to-end QoT, we only consider the failure of each link present in working path of considered backup path since backup path is enabled only when its working fails.

Once the required data rate is allocated, we stop this process without checking any further FSs in path 'p'. Then, Algorithm 3 returns the array Y (assigned FSs) to Algorithm 2 (line 29, Algorithm 3). Next, we focus on allocation of backup paths of considered working path (line 8, Algorithm 2).

2) ALLOCATION FOR BACKUP PATH

For each backup path, allocation is done by calling the Algorithm 4 (line 9, Algorithm 2) which follows the similar approach used for working path except the changes mentioned in Algorithm 4.

3) SELECTION OF WORKING AND BACKUP PATHS

Once the allocation is done in considered working path 'p' and one of its backup paths 'p_b', we find the value of objective function ($obj_{p,r}^{p_b}$, sum of highest indexed allocated FS in each link) by considering the spectrum allocations in 'p' and 'p_b' including the FSs assigned in p' and p'_b of R_{exi} (line 11, Algorithm 2). Next, we repeat the same process (described in previous subsection) for remaining backup paths (p_b) of working path 'p'. Note that, for each 'p' and its corresponding 'p_b' (if the allocation is successful in both paths), we compute the objective value $obj_{p,r}^{p_b}$ (line 11, Algorithm 2). Thus, we get $K * K_b$ possible objective values for considered request 'r'. Now, we choose the minimum objective function owing to selected working path 'p' and its corresponding backup path 'p_b' (lines 14-15, Algorithm 2) and process the next request.

If we cannot allocate the required spectrum either in all working paths or in all backup paths of each working path of a request, we block that request and process the next request.

C. COMPLEXITY ANALYSIS

The complexity of our proposed heuristic algorithm for static traffic scenario is $O(|C|^2|K||K_b||N||M||E|^2)$, where $|C|$, $|K|$, $|K_b|$, $|N|$, $|M|$ and $|E|$ are total number of requests, working paths (of one request), backup paths (of one working path), FSs in a link, MFs and links, respectively. Next, complexity of heuristic for each incoming request under dynamic traffic scenario is $O(|C'||K||K_b||N||M||E|^2)$, where $|C'|$ is the number of existing requests in the network. Further, complexity of our proposed sorting technique is $O(|C||K||K_b||E|)$.

VI. MILP AND HEURISTIC AUGMENTATION CONSIDERING INTER-CHANNEL CROSSTALK

In this section, we describe the RSA design for QoT ensured SBPP EON considering inter-channel crosstalk (ICC) along with in-band crosstalk (IXT), amplified spontaneous emission (ASE) and beating noise through MILP and the heuristic. To compute the ICC interference (ICCI), we use the Gaussian noise (GN) model presented in [29] and [37]. Noteworthy, interference calculation using GN model is inaccurate for bandwidth less than 28 GHz. Therefore, we consider 32 GBaud bandwidth variable transponders (BVTs) where each BVT provides 50 Gbps data rate (assuming dual polarization including 20% FEC overhead) for BPSK in a FS of 37.5 GHz (by combining three frequency slices each of 12.5 GHz) [38]. Based on GN model, ICCI on FS 'f' in link 'l' due to particular FS f' allotted to existing request r' is calculated as

$$ICCI_{f,l}^{r',f'} = \Omega \triangle b G(b) \left[G^2(b) \ln \left| \frac{\pi^2 \beta_2 (\triangle b)^2}{\alpha} \right| + G^2(b') \ln |\mu| \right]; \tag{51}$$

where,

$$\Omega = \frac{3\gamma^2}{2\pi\alpha|\beta_2|} \text{ and } \mu = \frac{|f - f'| + \triangle b'/2}{|f - f'| - \triangle b'/2};$$

'α', 'β_2' and 'γ' in above equation denotes the power attenuation, fiber dispersion and fiber nonlinear coefficient, respectively. $G(b)$ represents the power spectral density of the signal having 'b' and $\triangle b$ as center frequency and bandwidth, respectively. $\triangle b'$ denotes the other signal bandwidth with center frequency b'. Unlike IXT, ICC is a link phenomena where FSs in the same link causes interference to each other which again requires robust design to ensure the QoT in SBPP EON. Therefore, for MILP, we include the robust design constraints corresponding to ICC by modifying (using 51) the constraints in sections IV-9 to IV-11. We incorporate the similar modifications in Algorithm 3 and 4 to implement robust design corresponding to ICC for proposed heuristic. Above modifications provide the MILP and heuristic which enables the QoT guaranteed RSA against all considered PLIs including ICC.

VII. MILP AND HEURISTIC FOR SRLG FAILURE

In this section, we extend our MILP and heuristic (proposed for QoT guarantee against single link failures) to design QoT guaranteed RSA in SBPP EON against SRLG failures. SRLG is a group of links which share same physical location or which are subjected to a common risk. Therefore, whenever a particular SRLG fails, all the links belongs to that SRLG are failed. In this case, all the working paths of the requests that are present in each failed link are deactivated and corresponding backup paths should be activated. For this to happen, first, we calculate K shortest working paths for each request similar to link failure case. However, while calculating K_b shortest

backup paths for each working path, we make sure that all K_b paths are SRLG disjoint (which is link disjoint for link failure case) to corresponding working path. Therefore, each allocated working and backup path of a particular request are SRLG disjoint (link disjoint for link failure case) to each other. This causes major difference in the allocations between SRLG failure and link failure case. Next, as explained in section I and III-B, similar to link failure case, different SRLG failures results in different R_w and R_b in the network and hence interference power on any FS is a function of failed SRLG. Therefore, robust optimization based RSA is required in this case also. By implementing similar concepts applied for link failure case (such as failing one SRLG at a time, finding maximum possible or robust IXTI considering each SRLG failure scenario etc.) proposed MILP and heuristic in sections IV and V can also be extended for SRLG failure by incorporating few changes as given below.

1) e denotes SRLG

2) L denotes the set of SRLGs present in whole network

3) L/l_p should be changed to $L/SRLG_p$, where $SRLG_p$ denotes the set of SRLGs present in path p

4) $e \in l_p$ should be changed to $e \in SRLG_p$

5) Link disjoint constraint in section IV-6 should be changed to SRLG disjoint constraint which states that backup paths of two different requests can share the FSs if corresponding working paths are SRLG disjoint. For this purpose, variable l in (15) and (19) should be changed to e. Further, (15) in its original form should also present as MILP constraint.

6) Use the term SRLG failure in place of link failure.

VIII. RESULTS AND DISCUSSION

In this section, we analyze the performance of the proposed MILP and the heuristic algorithm through simulation results. In particular, we evaluate the MILP under static traffic conditions whereas the heuristic is examined for both static and dynamic traffic scenarios. For this purpose, we adopt a 6-node network for MILP evaluation and a 14-node network for heuristics as shown in Fig. 3 and 5(c), respectively. We assume that each link in considered networks is a bidirectional fiber and consists of 30 FSs in 6-node network and 320 FSs in 14-node network. Data rate of each request is chosen randomly following uniform distribution ranging from 10 to 70 Gbps for MILP and 10 to 700 Gbps for heuristics. Further, for each request, we compute $K = 3$ working paths and for each working path, we calculate $K_b = 3$ (wherever possible) backup paths which are link disjoint to corresponding working path. Next, we consider 4 different MFs namely BPSK, QPSK, 8-QAM and 16-QAM having approximate SINR thresholds 12.6 dB, 15.6 dB, 19.2 dB and 22.4 dB, respectively for a BER of 10^{-9} [27]. Note that, for each value of total traffic load, we conduct the experiment 30 times and average the results. We employed IBM CPLEX V12.6 and MATLAB 2020 for the implementation of MILP and heuristics, respectively. Simulation experiments are performed on Intel Core i7 3.4 GHz CPU with 8 GB RAM. Simulation parameters are given in Table 2 for broadcast and select (BS) node architecture [27].

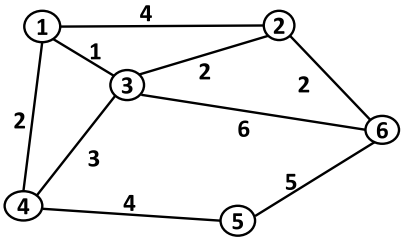

FIGURE 3. Sample 6-node network (link distance is in 100's of kilometers).

A. PERFORMANCE EVALUATION UNDER STATIC TRAFFIC SCENARIO

1) FOR SMALL NETWORK

We compare the MILP with the proposed heuristic SBPP-IA for the 6-node network (Fig. 3) considering the existing and proposed sorting techniques most data rate first (MDF) and MCW-LCBF, respectively in terms of optimality gap (G) as shown in Fig. 4. 'G' is the percentage deviation between MILP objective value and that of heuristic. Fig. 4 describes that 'G' increases with the increase in traffic load. Further, it is evident from Fig. 4 that our SBPP-IA employing proposed MCW-LCBF outperforms the existing MDF. This is because, according to MDF technique, request with highest data rate demand is established first. On the other hand, our proposed MCW-LCBF considers the probability of congestion in each working and backup path of every request and sorts the requests in such a way that there exists maximum benefit in the allocations of both working and backup paths as explained in section V-A. It is also to be noted that, value of 'G' is significantly less (less than 5%) for our proposed sorting technique and the heuristic even at higher loads.

2) FOR REALISTIC NETWORK

As MILP involves complex computations for large scale simulations, we analyze the performance of the proposed SBPP-IA for the 14-node network (Fig. 5(c)). In this regard, SBPP-IA employing MCW-LCBF and MDF are compared with respect to bandwidth blocking probability (BBP) and fragmentation as shown in 5(a) and 5(b), respectively. BBP is calculated by finding the ratio of total bandwidth of blocked requests and overall bandwidth of all requests. Further, fragmentation is calculated as [39]:

$$F_r = 1 - \frac{\text{largest continuous free FSs block}}{\text{total free FSs}} \tag{52}$$

As shown in Fig. 5, simulations are carried out for different values of crosstalk factor (C_x). Fig. 5(a) describes that BBP increases as traffic load increases. This is due to the effect of higher interference and insufficient resources with the increase in traffic load. Further, higher C_x value introduces higher interference which eventually increases the BBP at each load.

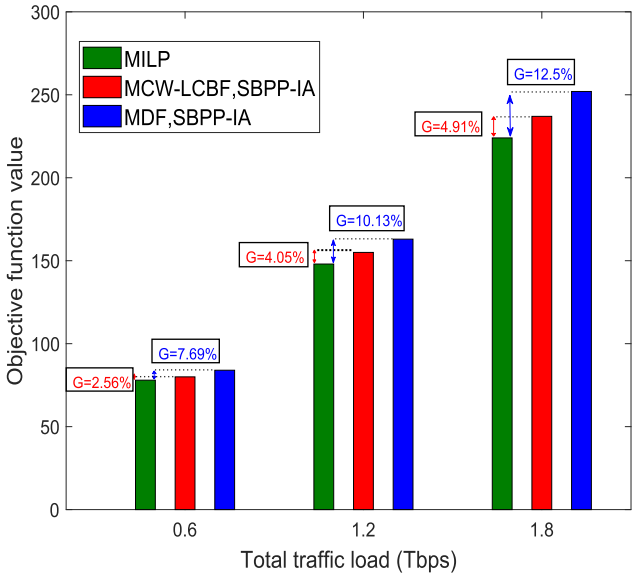

FIGURE 4. Comparison of heuristic with MILP with respect to Optimality gap (G) for a 6-node network at $C_x = -30$ dB, N=30.

When it comes to fragmentation, as BBP starts from 40 Tbps (Fig. 5(a)), we evaluate the performance of SBPP-IA in terms of fragmentation for the overall load of 5-35 Tbps as shown in Fig. 5(b). We observe that, similar to BBP, fragmentation also increases as traffic load and C_x increase. The reason is that, the increase in traffic load causes more interaction between the FSs of different requests introducing more interference at FSs and therefore not allowing any MF to be allocated. In that case, to minimize the effect of interference, requests are more fragmented during the allocation increasing overall fragmentation of the network.

It is interesting to observe that, our SBPP-IA employing the proposed sorting technique MCW-LCBF results in better performance in terms of BBP and fragmentation than the existing MDF technique (refer Fig. 5(a) and 5(b)). This is because, as mentioned before, MDF sorts the requests only based on the data rate requirement of each request whereas our MCW-LCBF takes the network congestion into account for better allocation.

B. PERFORMANCE EVALUATION UNDER DYNAMIC TRAFFIC SCENARIO

For dynamic traffic scenario, we assume that each request's arrival follows a Poisson process while holding times are negative exponentially distributed [17]. Here, we simulate 1,00,000 requests where the data rate demand of each request is chosen between 10-700 Gbps obeying uniform distribution. Algorithm 2 proposed in section V-B is used for the allocation of dynamic traffic. Though SBPP-IA heuristic presented in Algorithm 2 is designed for static traffic, it can also be also employed for dynamic traffic. This is because, for static traffic, after deciding the order in which each request is to be established, we allocate every request one by one by incorporating the lines 3-15 in Algorithm 2. Similarly, in case of dynamic traffic, we implement the lines 3-15 in Algorithm 2 to establish the incoming request during the arrival. Therefore, sorting of requests step presented in line 1 of Algorithm 2 is not required for dynamic traffic. Next, during the departure, allocated FSs in working and backup path of departed request are released which can be used to accommodate the future incoming requests. However, we do not release the backup FSs of departed request involved in sharing with existing requests.

TABLE 2. Simulation parameters.

Parameter	Value
LO power (P_{lo}), Received power (P_r)	0 dBm, -12 dBm
Responsivity (R_a), Operating frequency (f_c)	0.7 A/W, 193.1 THz
Spontaneous Emission factor (n_{sp})	2
Switch through loss (dB) assuming broadcast and select architecture [27]	3 $\lceil log_2 Q \rceil + L_{WSS}$, Q: inputs/outputs
Fiber attenuation (α), WSS loss (L_{WSS})	0.2 dB/km, 2 dB
Tap loss (L_{tap})	1 dB
EDFA spacing (E_s) [29]	100 km
Input EDFA gain (G_{in})	22 dB
Output EDFA gain (G_{out}) for 6-node (see Fig. 3)	5 dB at node 3, 8 dB elsewhere
Output EDFA gain (G_{out}) for 14-node (see Fig. 5(c))	5 dB at nodes 1, 14 11 dB at nodes 6, 9 8 dB elsewhere
Crosstalk factor (Cx)	[-30, -35 -40] dB
Electrical bandwidth (B_e)	7 GHz
Planck's constant (h)	6.62×10^{-34} J.s

Here, we compare the performance of our SBPP-IA heuristic with SBPP-spectrum window plane (SBPP-SWP) algorithm proposed in [17] in which distance adaptive RSA was designed for SBPP EON without considering the effect of PLIs. Noteworthy, after the design of distance adaptive SBPP-SWP algorithm in [17], various authors extended SBPP EON to different areas such as IP over EON, traffic grooming, multicast RSA etc. Therefore, to compare the performance of our proposed SBPP-IA algorithm for dynamic traffic, we use the standard distance adaptive algorithm (SBPP-SWP) proposed for SBPP EON in [17] as a benchmark. For this purpose, we simulate SBPP-IA and SBPP-SWP algorithms for the 14-node network (Fig. 5(c)) under dynamic traffic scenario.

First, we evaluate performance comparison between SBPP-IA and SBPP-SWP in terms of percentage of QoT failed requests. To calculate the percentage of QoT failed requests for SBPP-SWP, we simulate this algorithm and perform RSA for working and backup path of each request. Next, for a given total traffic load value, by failing one link in the network, we compute the percentage of QoT failed requests while considering PLIs. Note that, if either active working path or active backup path of any request is failed to meet minimum QoT requirements then the corresponding request is considered to be QoT failed request. We repeat this procedure for each single link failure and no link failure cases and corresponding results are plotted in Fig. 6(a). Due

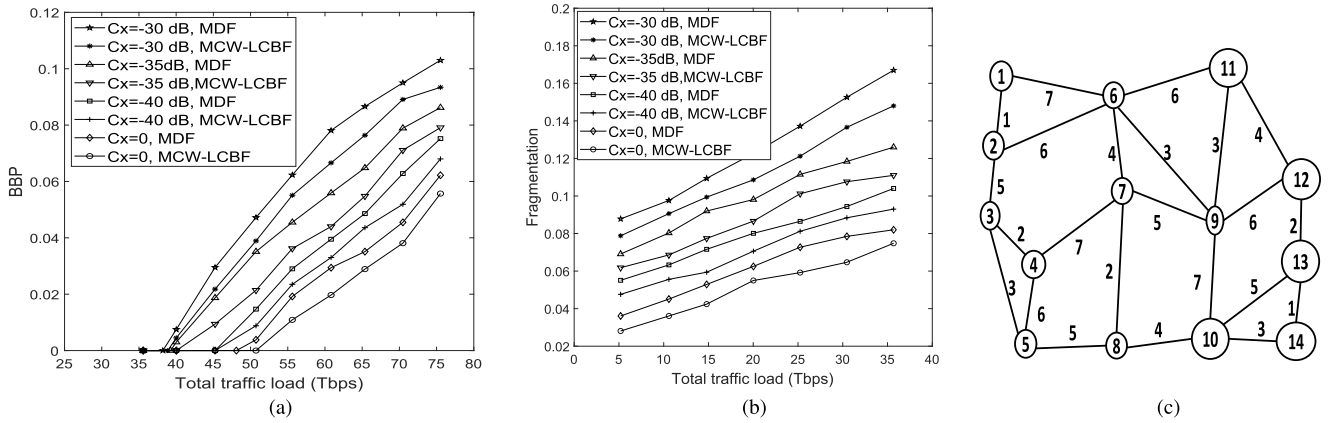

FIGURE 5. Performance evaluation of proposed SBPP-IA for different crosstalk factors (C_x) under static traffic scenario for 14-node network. (a) Bandwidth blocking probability (b) Fragmentation (c) 14-node network (link distance is in 100's of kilometers).

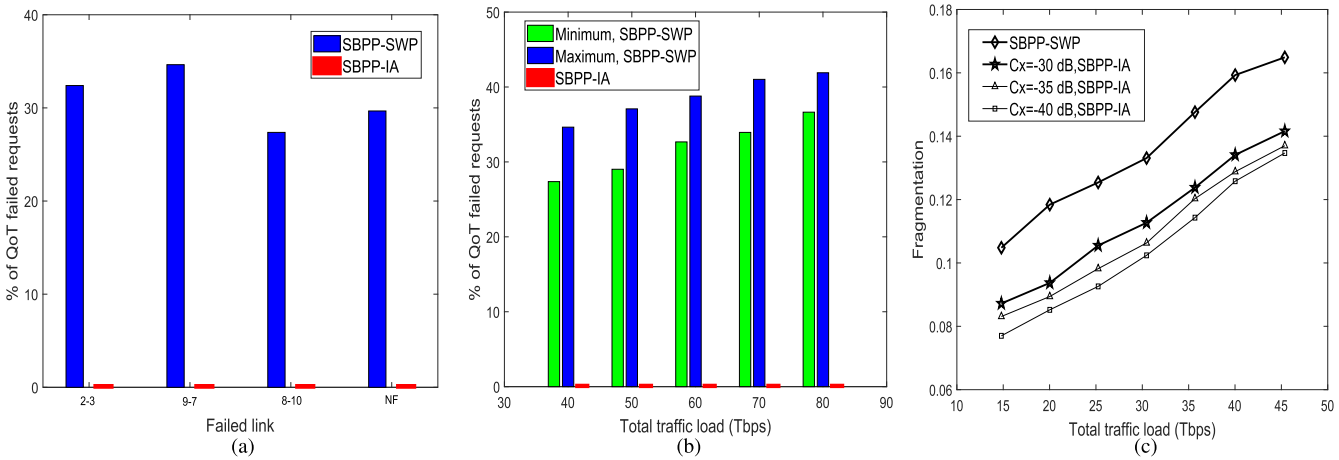

FIGURE 6. Performance comparison of proposed SBPP-IA with SBPP-SWP under dynamic traffic scenario for 14-node network at $C_x = -30$ dB. (a) Percentage of QoT failed requests for SBPP-SWP under different link failure scenarios at 40 Tbps network load (b) Maximum and minimum possible percentage of QoT failed requests for SBPP-SWP (c) Fragmentation.

to space constraint, we have shown results correspond to few single link failure cases and no link failure (denoted by NF on X-axis, Fig. 6(a)) case for a network load of 40 Tbps (Fig. 6(a)).

It is interesting to observe that, each single link failure results in different percentage of QoT failed requests which is again different for no link failure case as illustrated in Fig. 6(a). Therefore, at each traffic load, by considering each single link failure and no link failure conditions, we calculate the minimum and maximum possible percentage of QoT failed requests denoted by 'Minimum' and 'Maximum,' respectively as shown in Fig. 6(b). Finally, results in Fig. 6(b) summarize that significant amount of requests are failing to meet minimum QoT requirements at each traffic load if the allocation is done using SBPP-SWP algorithm in which the effect of PLIs are not considered. On the other hand, we observe that, our SBPP-IA algorithm guarantees minimum QoT assured allocation in both working and backup paths for each request under any single link failure and no link failure conditions at any traffic load.

Next, Fig. 6(c) and 7(a) describe that fragmentation and BBP increase with increase in load for SBPP-IA and SBPP-SWP algorithms. Further, performances in terms of BBP and fragmentation are improved in SBPP-IA as C_x reduces. When it comes to backup sharing, it is to be noted that, our proposed SBPP-IA attempts to minimize the fragmentation in each link which in turn offers maximum possible sharing among the backup FSs. To demonstrate this, we calculate the shareability at various traffic loads for different C_x values and the corresponding results are shown in Fig. 7(b). Shareability denotes the percentage of backup FSs involved in sharing among total allocated backup FSs and is calculated as follows:

$$\text{Shareability} = \frac{\sum_l \sum_f (s_{f,l} - 1)}{N_b} \times 100 \qquad (53)$$

where, $s_{f,l}$: Number of requests shared the FS *'f'* in link *'l'*, N_b : Number of backup FSs allocated in the network.

Results in Fig. 7(b) demonstrate that, shareability increases as traffic load grows since opportunities for sharing the backup FSs among requests get increased with increase in

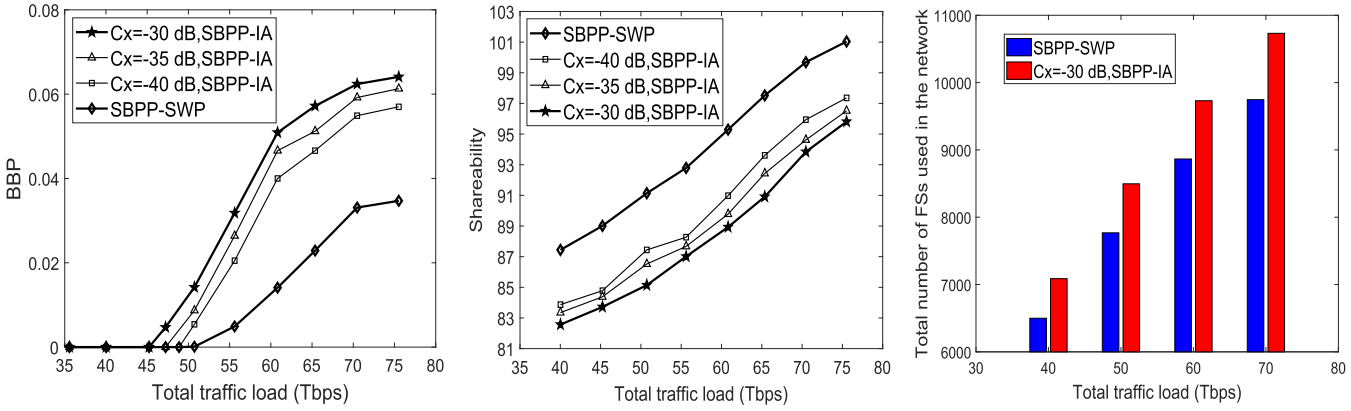

(a) (b) (c)

FIGURE 7. Performance comparison of proposed SBPP-IA with SBPP-SWP under dynamic traffic scenario for 14-node network. (a) BBP (b) Shareability (c) Total number of FSs used.

traffic load. Further, effect of crosstalk is also observed in Fig. 7(b) where backup shareability improves as C_x decreases. This is because, requests can be closely allocated in presence of less interference which increases the backup sharing. It is evident from Fig. 7(b) that our objective function achieves significant backup shareability in the network. In addition, shareability of SBPP-SWP algorithm at different loads is also presented in Fig. 7(b). Next, Fig. 7(c) depicts that, total number of FSs used in the network increases with increase in traffic load both in case of SBPP-IA and SBPP-SWP algorithms.

Now, we illustrate the performance comparison between SBPP-IA and SBPP-SWP in terms of fragmentation, BBP, shareability and total number of FSs used while considering $C_x = -30$ dB for SBPP-IA. For better readability, results corresponding to SBPP-IA ($C_x = -30$ dB) and SBPP-SWP are represented with bold lines as in Fig. 6(c), 7(c) and 7(b). It is observed that, SBPP-SWP shows better performance than our SBPP-IA algorithm in terms of BBP, shareability and total number of FSs used (refer Fig. 7). This is due to the effect of PLIs considered in our algorithm during the allocation. However, this performance difference is not significant due to the following reasons. Firstly, we employ the efficient spectrum allocation technique named bitloading in our robust RSA design. Secondly, RSA was performed in such a way that overall fragmentation in the network is minimized. On the other hand, our SBPP-IA outperforms the SBPP-SWP in terms of percentage of QoT failed requests and fragmentation as shown in Fig. 6(b) and 6(c), respectively.

For better understanding, we observe our results at 70 Tbps total traffic load (Fig. 6 and 7) to compare SBPP-IA and SBPP-SWP. At 70 Tbps, SBPP-SWP performs slightly better compared to SBPP-IA by a percentage of 2.93, 5.85 and 6.12 in terms of BBP, shareability and total number of FSs used, respectively. Conversely, our SBPP-IA outperforms SBPP-SWP by a percentage of 33.94-41.02 (depending upon location of link failure) and 2.33 in terms of QoT failed requests and fragmentation, respectively.

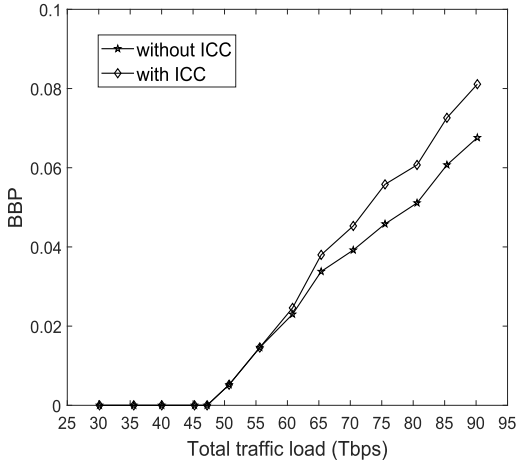

FIGURE 8. Performance of proposed SBPP-IA under dynamic traffic with and without ICC for 14-node network in terms of BBP.

C. PERFORMANCE EVALUATION OF HEURISTIC CONSIDERING INTER-CHANNEL CROSSTALK

In this section, we investigate the performance of proposed heuristic in terms of BBP by taking ICC into account in addition to IXT, ASE and beating noise. Fiber dispersion (β_2) and nonlinear coefficient (γ) values for adopted Gaussian model to calculate ICCI [29] are $-21.7\ ps^2/km$ and $1.33\ W^{-1}km^{-1}$, respectively. As shown in Fig. 8, simulations are carried out for RSA design with and without ICC. Note that, in the case of "with ICC", we considered ICC, IXT, ASE and beating noise in RSA design where as in "without ICC" case, we took IXT, ASE and beating noise only into account. As can be seen in Fig. 8, performance of BBP is same at lower loads in case of "with ICC" and "without ICC". This is because, at lower loads, there exists enough space in the spectrum for connections to get separated to avoid interference due to ICC. On the other hand, at higher loads, BBP is degraded in case of "with ICC" compared to "without ICC" due to interference and fragmentation.

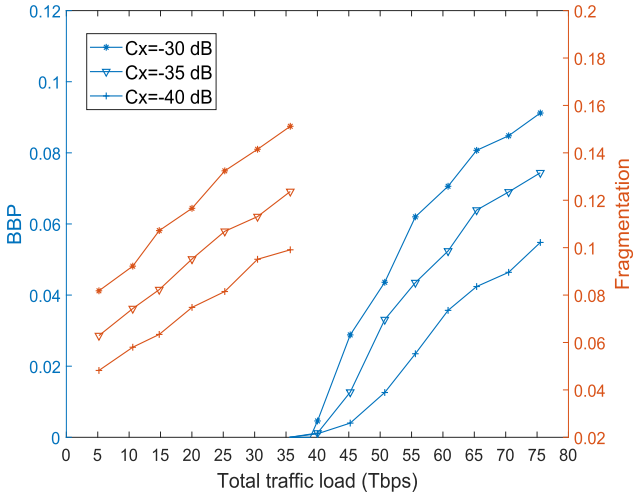

FIGURE 9. Performance of proposed SBPP-IA using MCW-LCBF sorting technique against node failure scenario under static traffic for 14-node network in terms of BBP and fragmentation.

D. PERFORMANCE EVALUATION OF HEURISTIC FOR SRLG FAILURE CASE

In this section, we examine the proposed heuristic (refer section VII) against SRLG failure for static traffic scenario. Note that, we simulated the heuristic and generated results considering the network node as SRLG for the 14-node network shown in 5(c). Further, for each request, we calculate $K = 3$ working paths and for each working path, we compute $K_b = 3$ (wherever possible) backup paths which are node disjoint to corresponding working path. If there exists no node disjoint paths for each working path of a request, we block that particular request. We evaluate the performance of heuristic in terms of BBP and fragmentation as shown in Fig. 9. As can be seen in Fig. 9, graphs follow similar pattern as in Fig. 5, 6 and 7 with the variation of load and C_x due to the same reason described for earlier results.

IX. CONCLUSION

In this paper, we focused on robust design of SBPP based EON which provides a minimum QoT assured RSA against PLIs under any single link/SRLG failure for static and dynamic traffic scenarios. In this regard, we considered PLIs such as IXT along with ASE and beating noise terms in our RSA design. Next, we formulated an MILP for smaller networks and proposed MCW-LCBF sorting technique followed by the SBPP-IA heuristic for larger networks under static traffic scenario. Results demonstrated that, our MCW-LCBF outperforms widely used existing MDF in terms of optimality gap, BBP and fragmentation. For dynamic traffic, our proposed SBPP-IA algorithm ensured the QoT of existing requests during the allocation of each new request without reserving any margin. Next, we compared our SBPP-IA algorithm with the existing SBBP-SWP algorithm in terms of different performance metrics. It is evident from simulation results that, though the minimum QoT assured resource allocation is an important attribute of optical network, existing SBPP-SWP results in significant QoT failed requests whereas our proposed SBPP-IA guarantees 100% QoT assured allocation in working and backup paths under any single link failure and no link failure conditions by compromising a little in terms of BBP, shareability and total number of FSs used.

APPENDIX
LINEARIZATIONS

1) Logical AND: $Z = XY$ can be linearized as given below
$Z \geq 0; Z \leq X; Z \leq Y; Z \geq X + Y - 1;$
2) Maximum of continuous variables:
$Y = max(X_1, X_2, \ldots, X_n)$ can be linearized as follows:
$L_i \leq X_i \leq U_i\,;\ \forall i = \{1, 2, \ldots, n\}$
$Y \geq X_i\,;\ \forall i$
$Y \leq X_i + (U_{max} - L_i)(1 - D_i)\,;\ \forall i$
$\sum_{i=1}^{n} D_i = 1\,;$
Where, L_i and U_i are lower and upper bounds of X_i, respectively, $U_{max} = max(U_1, U_2 \ldots . U_n)$. In our case, $L_i = 0$, $U_i = \left\lceil \frac{N_d - 2}{2} \right\rceil \times N_{xc} \times P_r \times C_x, \forall i$
Where, N_d = maximum nodal degree in the network, N_{xc} = total number of nodes in the network.
Further, we define $D_1, D_2, \ldots, D_n$ as binary variables for which $D_i = 1$ if X_i is the maximum value, 0 otherwise.

REFERENCES

[1] B. C. Chatterjee, S. Ba, and E. Oki, "Fragmentation problems and management approaches in elastic optical networks: A survey," *IEEE Commun. Surveys Tuts.*, vol. 20, no. 1, pp. 183–210, 1st Quart., 2017.
[2] G. Shen, H. Guo, and S. K. Bose, "Survivable elastic optical networks: Survey and perspective," *Photon. Netw. Commun.*, vol. 31, no. 1, pp. 71–87, Feb. 2016.
[3] G. Shen, Y. Wei, and S. K. Bose, "Optimal design for shared backup path protected elastic optical networks under single-link failure," *IEEE/OSA J. Opt. Commun. Netw.*, vol. 6, no. 7, pp. 649–659, Jul. 2014.
[4] N. G. Anoh, M. Babri, A. D. Kora, R. M. Faye, B. Aka, and C. Lishou, "An efficient hybrid protection scheme with shared/dedicated backup paths on elastic optical networks," *Digit. Commun. Netw.*, vol. 3, no. 1, pp. 11–18, Feb. 2017.
[5] H. Guo, G. Shen, and S. K. Bose, "Routing and spectrum assignment for dual failure path protected elastic optical networks," *IEEE Access*, vol. 4, pp. 5143–5160, 2016.
[6] A. Cai, J. Guo, R. Lin, G. Shen, and M. Zukerman, "Multicast routing and distance-adaptive spectrum allocation in elastic optical networks with shared protection," *J. Lightw. Technol.*, vol. 34, no. 17, pp. 4076–4088, Sep. 1, 2016.
[7] W. Lu, X. Yin, X. Cheng, and Z. Zhu, "On cost-efficient integrated multilayer protection planning in IP-over-EONs," *J. Lightw. Technol.*, vol. 36, no. 10, pp. 2037–2048, May 6, 2018.
[8] P. Papanikolaou, K. Christodoulopoulos, and E. Varvarigos, "Joint multi-layer survivability techniques for IP-over-elastic-optical-networks," *J. Opt. Commun. Netw.*, vol. 9, no. 1, p. A85, 2017.
[9] S. Yin, S. Huang, B. Guo, Y. Zhou, H. Huang, M. Zhang, Y. Zhao, J. Zhang, and W. Gu, "Shared-protection survivable multipath scheme in flexible-grid optical networks against multiple failures," *J. Lightw. Technol.*, vol. 35, no. 2, pp. 201–211, Jan. 15, 2017.
[10] W. Wang and J. Doucette, "Availability optimization in shared-backup path protected networks," *J. Opt. Commun. Netw.*, vol. 10, no. 5, pp. 451–460, 2018.

[11] B. Chen, J. Zhang, Y. Zhao, J. P. Jue, S. Huang, W. Gu, and G. Shen, "Spectrum-aware survivable strategies with failure probability constraints under static traffic in flexible bandwidth optical networks," *J. Lightw. Technol.*, vol. 32, no. 24, pp. 4221–4234, Nov. 1, 2014.

[12] J. Wu, Z. Ning, and L. Guo, "Energy-efficient survivable grooming in software-defined elastic optical networks," *IEEE Access*, vol. 5, pp. 6454–6463, 2017.

[13] F. Tang, W. Shao, L. Xiang, S. K. Bose, and G. Shen, "Mixed channel traffic grooming for IP over EON with SBPP-based cross-layer protection," *J. Lightw. Technol.*, vol. 35, no. 18, pp. 3836–3848, Sep. 15, 2017.

[14] E. E. Moghaddam, H. Beyranvand, and J. A. Salehi, "Routing, spectrum and modulation level assignment, and scheduling in survivable elastic optical networks supporting multi-class traffic," *J. Lightw. Technol.*, vol. 36, no. 23, pp. 5451–5461, Dec. 1, 2018.

[15] J. Halder, T. Acharya, M. Chatterjee, and U. Bhattacharya, "On spectrum and energy efficient survivable multipath routing in off-line elastic optical network," *Comput. Commun.*, vol. 160, pp. 375–387, Jul. 2020.

[16] B. Chen, J. Zhang, Y. Zhao, J. P. Jue, J. Liu, S. Huang, and W. Gu, "Spectrum–block consumption for shared-path protection with joint failure probability in flexible bandwidth optical networks," *Opt. Switching Netw.*, vol. 13, pp. 49–62, Jul. 2014.

[17] C. Wang, G. Shen, and S. K. Bose, "Distance adaptive dynamic routing and spectrum allocation in elastic optical networks with shared backup path protection," *J. Lightw. Technol.*, vol. 33, no. 14, pp. 2955–2964, Jul. 15, 2015.

[18] A. L. Ferraz Lourenço and A. C. César, "Algorithm for shared path protection in elastic optical network based on spectrum partition," in *IEEE MTT-S Int. Microw. Symp. Dig.*, Aug. 2017, pp. 1–5.

[19] X. Luo, C. Shi, L. Wang, X. Chen, Y. Li, and T. Yang, "Leveraging double-agent-based deep reinforcement learning to global optimization of elastic optical networks with enhanced survivability," *Opt. Exp.*, vol. 27, no. 6, pp. 7896–7911, Mar. 2019.

[20] C.-F. Hsu, H.-C. Hu, H.-F. Fu, J.-J. Zheng, and S.-X. Chen, "Spectrum usage minimization for shared backup path protection in elastic optical networks," in *Proc. Int. Conf. Comput., Netw. Commun. (ICNC)*, Feb. 2019, pp. 602–606.

[21] N. Jara, H. Pempelfort, G. Rubino, and R. Vallejos, "A fault-tolerance solution to any set of failure scenarios on dynamic WDM optical networks with wavelength continuity constraints," *IEEE Access*, vol. 8, pp. 21291–21301, 2020.

[22] A. Fontinele, I. Santos, J. N. Neto, D. R. Campelo, and A. Soares, "An efficient IA-RMLSA algorithm for transparent elastic optical networks," *Comput. Netw.*, vol. 118, pp. 1–14, May 2017.

[23] B. C. Chatterjee, N. Stol, and E. Oki, "Impairment-aware spectrum allocation in elastic optical networks: A dispersion-sensitive approach," *Opt. Fiber Technol.*, vol. 61, Jan. 2021, Art. no. 102431.

[24] Y. Zhou, Q. Sun, and S. Lin, "Link state aware dynamic routing and spectrum allocation strategy in elastic optical networks," *IEEE Access*, vol. 8, pp. 45071–45083, 2020.

[25] J. Zhao, B. Bao, H. Yang, E. Oki, and B. C. Chatterjee, "Holding-time-and impairment-aware shared spectrum allocation in mixed-line-rate elastic optical networks," *J. Opt. Commun. Netw.*, vol. 11, no. 6, pp. 322–332, 2019.

[26] S. Behera, J. George, and G. Das, "Effect of transmission impairments in CO-OFDM based elastic optical network design," *Comput. Netw.*, vol. 144, pp. 242–253, Oct. 2018.

[27] S. Behera, A. Deb, G. Das, and B. Mukherjee, "Impairment aware routing, bit loading, and spectrum allocation in elastic optical networks," *J. Lightw. Technol.*, vol. 37, no. 13, pp. 3009–3020, Jul. 1, 2019.

[28] R. Wang, S. Bidkar, F. Meng, R. Nejabati, and D. Simeonidou, "Load-aware nonlinearity estimation for elastic optical network resource optimization and management," *J. Opt. Commun. Netw.*, vol. 11, no. 5, pp. 164–178, 2019.

[29] J. Zhao, H. Wymeersch, and E. Agrell, "Nonlinear impairment-aware static resource allocation in elastic optical networks," *J. Lightw. Technol.*, vol. 33, no. 22, pp. 4554–4564, Nov. 15, 2015.

[30] R. Krishnamurthy and T. Srinivas, "Physical layer impairments aware routing and spectrum allocation algorithm for transparent flexible-grid optical networks," *Comput. Commun.*, vol. 153, pp. 507–514, Mar. 2020.

[31] V. A. C. Vale and R. C. Almeida, "Power, routing, modulation level and spectrum assignment in all-optical and elastic networks," *Opt. Switching Netw.*, vol. 32, pp. 14–24, Apr. 2019.

[32] F. I. Calderón, A. Lozada, D. Bórquez-Paredes, R. Olivares, E. J. Davalos, G. Saavedra, N. Jara, and A. Leiva, "BER-adaptive RMLSA algorithm for wide-area flexible optical networks," *IEEE Access*, vol. 8, pp. 128018–128031, 2020.

[33] B. Ramamurthy, D. Datta, and H. Feng, "Impact of transmission impairments on the teletraffic performance of wavelength-routed optical networks," *J. Lightw. Technol.*, vol. 17, no. 10, p. 1713, Oct. 1999.

[34] D. Datta, *Optical Networks*. Oxford, U.K.: Oxford Univ. Press, 2022.

[35] Y. Wang, X. Cao, and Y. Pan, "A study of the routing and spectrum allocation in spectrum-sliced elastic optical path networks," in *Proc. IEEE INFOCOM*, Apr. 2011, pp. 1503–1511.

[36] M. Jinno, B. Kozicki, H. Takara, A. Watanabe, Y. Sone, T. Tanaka, and A. Hirano, "Distance-adaptive spectrum resource allocation in spectrum-sliced elastic optical path network [topics in optical communications]," *IEEE Commun. Mag.*, vol. 48, no. 8, pp. 138–145, Aug. 2010.

[37] P. Johannisson and E. Agrell, "Modeling of nonlinear signal distortion in fiber-optic networks," *J. Lightw. Technol.*, vol. 32, no. 23, pp. 4544–4552, Dec. 1, 2014.

[38] M. Song, E. Pincemin, A. Josten, B. Baeuerle, D. Hillerkuss, J. Leuthold, R. Rudnick, D. M. Marom, S. Ben Ezra, J. F. Ferran, G. Thouenon, P. S. Khodashenas, J. M. Rivas-Moscoso, C. Betoule, D. Klonidis, and I. Tomkos, "Flexible optical cross-connects for high bit rate elastic photonic transport networks," *J. Opt. Commun. Netw.*, vol. 8, no. 7, p. A126, 2016.

[39] P. R. Wilson, M. S. Johnstone, M. Neely, and D. Boles, "Dynamic storage allocation: A survey and critical review," in *Proc. Int. Workshop Memory Manage.* Cham, Switzerland: Springer, 1995, pp. 1–116.

VENKATESH CHEBOLU received the Master of Technology degree from the Electronics and Communication Department, National Institute of Technology, Rourkela, India, in 2015. He is currently pursuing the Ph.D. degree with the G. S. Sanyal School of Telecommunications, Indian Institute of Technology, Kharagpur, India. His research interests include optical backbone networks, survivability in elastic optical networks, and cross-layer optimization.

SADANANDA BEHERA received the Master of Technology degree from the Electronics and Communication Department, National Institute of Technology, Rourkela, India, in 2014, and the Ph.D. degree from the G. S. Sanyal School of Telecommunications, Indian Institute of Technology, Kharagpur, India. He is currently working as a Postdoctoral Researcher at the KIOS Research and Innovation Center of Excellence, University of Cyprus, Cyprus. His research interests include optical backbone networks, elastic optical networks, survivability of data plane and SDN-based control plane in EON, and cross-layer optimization.

GOUTAM DAS (Member, IEEE) received the Ph.D. degree from the University of Melbourne, Australia, in 2008. He has worked as a Postdoctoral Fellow at Ghent University, Belgium, from 2009 to 2011. Currently, he is working as an Associate Professor at the Indian Institute of Technology, Kharagpur, India. His research interests include optical access networks, optical data center networks, radio over fiber technology, elastic optical networks, optical packet switched networks, and media access protocol design for application specific requirements.